Journal of Sound and Vibration 459 (2019) 114865

Contents lists available at ScienceDirect

Journal of Sound and Vibration

journal homepage: www.elsevier.com/locate/jsvi

A review of particle damping modeling and testing

Louis Gagnon [a,*], Marco Morandini [b], Gian Luca Ghiringhelli [b]

[a] Institute of Aerodynamics and Gas Dynamics, University of Stuttgart, 70569, Stuttgart, Germany
[b] Department of Aerospace Science and Technology, Politecnico di Milano, 20156, Milano, Italy

ARTICLE INFO

Article history:
Received 21 December 2018
Revised 23 July 2019
Accepted 24 July 2019
Available online 27 July 2019
Handling Editor: H. Ouyang

Keywords:
Discrete element method
Distinct element method
Experimental testing
Granular structure
Numerical modeling
Particle damping
Particle dynamics

ABSTRACT

This survey provides an overview of the different approaches seen in the literature concerning particle damping. The emphasis is on particle dampers used on beams vibrating at frequencies between 10 Hz and 1 kHz. Design examples, analytical formulations, numerical models, and experimental setups for such dampers are gathered. Modeling approaches are presented both for particle interaction and for systems equipped with particle dampers. The consequences of the nonlinear behavior of particle dampers are brought to attention. As such, the apparent contradictions of the conclusions and approaches presented in the literature are highlighted. A list of particle simulation software and their use in the literature is provided. Most importantly, a suggested approach to create a sound numerical simulation of a particle damper and the accompanying experimental tests is given. It consists of setting up a discrete element method simulation, calibrating it with literature data and a representative damper experiment, and testing it outside of the range of operation used for the tuning.

1. Introduction

Particle dampers are devices that work by a combination of impact and friction damping. They dissipate the energy of a system by transferring it to a bed of particles. This bed is geometrically constrained to remain inside a container fixed to the vibrating system. As such, the motion-caused interaction occurring inside the container damps the absorbed energy. The main dissipative mechanisms involved are: collisions between the container walls and the particles and between the particles themselves; sliding friction between the same; and, rolling friction between the same. For collisions between the particles and the cavity walls to occur, both should be out-of-phase with each other. This type of damping mechanism allows for relatively empty containers, can work at low frequencies. Its optimization often focuses on the travel time of the particles within the cavity. This damping mechanism is often linked to the work of Masri and Ibrahim [1]. Another important mechanism that is active inside particle dampers relates to the state of matter of the granular medium. For example, gas-like states occur at higher frequencies and solid and liquid-like states occur at lower frequencies and excitation amplitudes. The optimization of that damping mechanism focuses on the state of the vibrated granules in the cavity. An original work along this line of thinking is that of Salueña et al. [2].

Particle damping is also referred to as *acceleration damping*, *multiple impact damping*, *multi-particle damping*, *granular damping*, *granular-fill damping*, and *shot damping*. Their invention stems from impact dampers, which work similarly but with a single particle. Typically, particle dampers are more efficient than the latter [3]. Both damper concepts are shown in Fig. 1, where u_{vib} is the transmitted vibrating motion.

* Corresponding author.
E-mail addresses: gagnon@iag.uni-stuttgart.de (L. Gagnon), marco.morandini@polimi.it (M. Morandini), gianluca.ghiringhelli@polimi.it (G.L. Ghiringhelli).

https://doi.org/10.1016/j.jsv.2019.114865

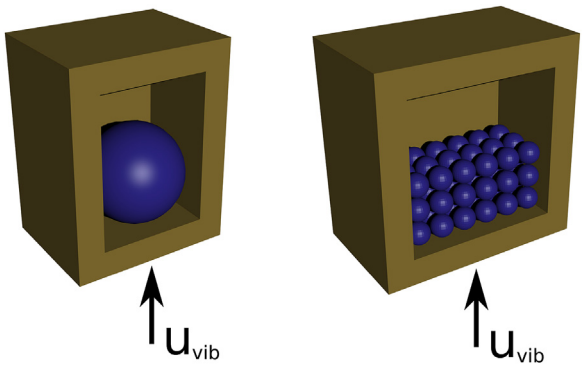

Fig. 1. Impact (left) and particle (right) dampers.

Particle dampers exhibit a number of advantages. They are particularly useful in harsh conditions, negligibly sensitive to oil contamination, and have a low weight impact [4]; are insensitive to the ambient temperature [5–7]; can work in multiple directions and at a wide range of frequencies [8]; operate without any source of power; can be designed to have low sensitivity to excitation in directions other than the principal one [9]; are efficient at damping either random, Gaussian, or deterministic excitation [3]; do not suffer from wear [6,7]; and, are simple, highly reliable, and affordable [6]. These characteristics make them particularly useful in harsh environments, in situations where electric or hydraulic power cannot be transmitted, and where vibrations are chaotic.

They are used in the aerospace, automotive, energy, and medical industries [10]. Applications include but are not limited to: earthquake isolation for buildings; engine oil pans; gears; aircraft components; turbine vanes and blades; spacecraft components; helicopter blades; turning machines and machine tools; wind turbines and wind-subjected pylons; and, aeronautical turbines. They are also considered to reduce the emission of sound [11] although sometimes they increase it [3]. They can be categorized based on their peculiarities and a sample of particle damper typology is:

- **single unit**: the typical particle damper which has a single cavity and is externally attached to the main structure;
- **multi-unit**: a particle damper which consists of more units attached to the main structure;
- **non-obstructive particle damper (NOPD)**: damper which does not modify the geometry of the main structure and often consists of one or more holes drilled into the structure;
- **tuned particle damper (TPD)**: classic dynamic vibration absorber which uses a cavity filled with particles instead of a mass;
- **vacuum packed particles (VPP)**: controllable pressure inside the particle cavity allows to actively control the response of the particle damper;
- **fine particle impact damper (FPID)**: a traditional impact damper where the large single impacting mass is placed in a cavity together with many smaller particles to increase energy dissipation.

Also, various levels of active control can be applied to particle dampers. Thus, the particle damper can either be passive, semi-active, or active [3]. The level of active control that will determine to which of the last two categories it belongs is not standardized and depends on subjective interpretations.

The scope of the current work is to present detailed descriptions of a selection of research items. The literature on particle damper is considerable and thus only papers which were similar enough to beam applications are presented in this paper. The reader will note that multiple applications are nevertheless presented and that the conclusions of this review can be extrapolated to other types of structures. The selection is thus based on the pertinence for damping beam vibrations between 10 Hz and 1 kHz. Priority is given to passive single-unit devices and descriptions of both numerical and experimental methods used by specific authors are reported. Most of the attention is given to dampers which dissipate energy through impact, as in the original work of Masri and Ibrahim [1]. These dampers are usually more effective and correspond to the solid state of dampers analyzed using a state of matter approach. This survey thus provides a complement, tailored to the aforementioned applications, to the recent particle damper review for civil engineering applications [12].

First, an overview of particle damper modeling and testing is given in Section 2. Section 3 introduces related analytical and numerical methods. Section 4 is dedicated to the considerations necessary for particle damper analysis with the discrete element method. Then, a series of configurations studied by different authors are given in Section 5. Finally, Section 6 suggests modeling and experimental approaches along with justifications.

2. Introductory considerations for modeling and testing

The literature repeatedly states that particle damping is a highly nonlinear phenomenon. Consequently analytical, numerical, and sometimes experimental studies on the subject present contradicting conclusions. As a matter of fact, most of the historical

research on particle dampers was conducted by trial and error [8]. There are thus many different approaches to their modeling and the specific configuration influences which internal mechanisms are important. This section introduces some peculiarities of particle dampers modeling and experimental testing.

Michon et al. [8] report that the highly nonlinear behavior of these dampers delayed and limited the use of analytical and numerical methods until the 1960s. They are still not yet well understood, and this even when operating under optimal conditions [13]. Quite often analytical approaches of the literature focus on damping a single mode of the structure, through an equivalent single degree of freedom (DoF) system. Many particle damper models from the literature suffer from the following limitations [8]: they often consider the particle aggregate as a lumped mass, they neglect internal friction, and they do not correct for the changes in the mass of the main structure caused by the particles being in contact or not with it.

Different directions of the observed vibrations will yield different optimal particle mass and damping properties [9,14]. Parasitic vibrations in secondary directions can also be strongly influential for dampers where the dissipation mechanism depends on the state of matter of the granular material. Multi DoF systems will respond differently than single DoF systems to the presence of the damper and gravity has a non-negligible effect on the damping [3]. The position of the particle damper on the response of the structure has a non-negligible influence on its effectiveness [9]. Also, the presence of a particle damper will usually increase the band of resonant frequencies while diminishing the peak response [15].

For one, it is common to obtain a single mass that is equivalent to a bed of particles. As such, the modeling is done using the obtained equivalent impact damper. Different formulations are available to do the conversion [4,16,17]. That single-mass approach can give a good estimation of the particle bed interaction with the containing structure. However, it fails to properly model the internal interaction between the particles [18]. This interaction induces dissipation caused by impact and friction phenomena. And, the dominant damping can come from either sliding or rolling friction or from impact dissipation [14,18]. For example, the experimentally validated numerical simulations of Wong et al. [19] indicate that the most important contribution of damping comes from friction. However, in general, the dominant dissipation mechanism is determined by the properties of the particles and their containing cavity [14].

In general, increasing the inelastic deformation of the particles increases the damping capability. But often, stiffer material coatings also lead to better damping [3]. The use of honeycomb beams can also improve the efficiency of the damping by providing many cavities that can be filled by particles. Most often, particle dampers use high density material granules [7]. Brown [20] mentions that a damper weighing between 10% and 15% of the effective system mass at the fundamental frequency is usually enough to achieve significant damping. In accordance, the mass ratio of the particles to the host system for all the simulations done by Sánchez et al. [10] remains $\approx 10\%$. Although increasing the mass ratio generally increases the performance of the damper, heavier dampers do not always translate into more damping at all modes because the state of the vibration is also important [3]. For example, the phase between the motion of the impacting mass and the structure to be damped has an important influence on the damping efficiency. Two impacts per cycle are more efficient and most of the damping usually occurs at or near resonance [3]. Because of their nature, particle dampers provide no damping once the oscillation amplitude goes under a certain level.

Furthermore, dividing the cavity into different compartments can prevent particles from aggregating and delay their response [9]. Fragmentation, or breaking, of the particles is numerically demonstrated not to limit the efficiency of the damper [10]. It is also advanced that as particles become smaller, the contact area between the vibrating part and the damper increases and thus promotes the exchange of momentum [3]. This mechanism is valid up to a lower limit on the size of the particles. Also, discrete element method (DEM) simulations showed that the properties of the individual grains of the particle damper have little influence on its damping properties if the optimal cavity clearance is maintained [21]. On the other hand, welding of individual particles can reduce the damper's efficiency [10].

2.1. Phase diagram analyses

The papers reported in this review are not separated based on whether they study the damping mechanism using a solid-fluid-gas phase perspective for the granular material. In this section, the term phase refers to the state of matter of the material. When the particles behave more like a gas, particle to wall impacts are usually dominant. However, the best damping is usually obtained for granular material in the solid, or glass, phase. Liquid-sloshing dampers are also not considered.

Nevertheless, a considerable amount of particle damper research focuses on the state of the granular material in the damper. These states are often referred to as solid or glass-like, liquid, or gaseous [22,23]. Consequently, the particles can also be modeled as two-phase flows [7]. Sometimes the distinction of phase is rather made between frictionless, frictional sliding, and rolling phases [24] or more detailed descriptions of the actual state of the flow [25,26]. Most often the phase of the granular material depends on both the excitation frequency and amplitude. Different phases observed also include bouncing bed, undulation, buoyancy convection, Leidenfrost effect, oscillons, waves, sloshing, and others. Credit for phase analysis of particle-induced energy dissipation is given to the research of Salueña et al. [2]. On a similar line of thought, Cates et al. [27] argues that the solid states of granular particles may be compared to fragile materials. The fragility of the granular material is linked to its ability to jam in a certain configuration where force chains are able to sustain loads up to a compatibility limit and at the same time may collapse due to an infinitesimal load applied in the proper direction. Such a collapse does not induce a flow state in the material but rather a plastic rearrangement of the particles.

The consideration for the phase state of granular flows leads to the use of diverse semi-active damper control techniques. These techniques aim to maintain a pressure on the boundaries of the cavity in order to favor the preservation of the solid particle arrangement and thus maintain good damping properties. The research in that direction considers the influence of the shape and aspect ratio of the cavity or the use of internal cellular structures, pressure-generating envelopes, or boundary electromagnets [28,29]; sandwich beam arrangements with controllable internal vacuum particle-filled flexible cavities [30,31]; and, flexible tube-like low-pressure granule-filled cavities [32].

2.2. Key terms

To clarify a few concepts, the following terms which recur in the particle damper literature are defined here:

- **mass ratio**: ratio of the mass of the damper to the mass of the vibrating structure[1];
- **Hooke contact**, **linear contact**: force between the particles is function of the displacement;
- **Hertz contact**: normal force between the particles is function of the displacement to the power of 3/2;
- **Kuwabara-Kono law**: normal damping force between the particles is function of the velocity times the square root of the penetration depth as defined by Kuwabara and Kono [33];
- **Hertz-Mindlin contact**: extension the Hertz contact model to have tangential components;
- **clearance**: refers to the distance that the particle(s) can travel from their initial position and is mostly used for impact dampers;
- **packing fraction**, **packing density**, **particle filling ratio**, **filling rate**: ratio of the space occupied by the particles to the space of the containing cavity[2];
- **bulk density**: ratio of the total mass of the particles to their volume envelope;
- **void fraction**, **mean voidage**, **porosity**: ratio of volume not occupied by particles to bulk volume of the particle aggregate;
- **void ratio**: within the aggregate, ratio of volume not occupied by particles to volume occupied by particles;
- **coefficient of internal friction**: Coulomb-type coefficient that characterizes the relation between the shear stress inside a particle bed and the normal stress [34]; strongly depends on void fraction;
- **coefficient of wall friction**: Coulomb-type coefficient that characterizes the relation between the shear stress on the particle bed wall and normal stress [34]; does not depend on void fraction but can be strongly influenced by vibrations;
- **clump**: bundle of bonded spheres which has the purpose of representing a particle of a specific shape for numerical simulation;
- **blockiness**: a number which indicates the proportion of sharp edges and corners versus rounded edges in a particle;
- **rolling resistance**, **rolling friction**: dry friction force dependent on normal contact force and opposing particle rolling motion;
- **coordination number**: the number of particles with which each particle is in contact[3];
- **granular shear strength**, **bulk friction**, **internal friction**: difference between the major and minor principal stresses in the granular material;
- **phenomenological model**: empirical model of a system which is only partly based on the principles of physics.

3. Modeling approaches

In order to calculate the response of a system equipped with a particle damper one can rely on analytical or numerical methods. Pure analytical methods for particle dampers are not common, are limited to specific cases, and are difficult to calibrate without having experimental data at hand. The Hertz formulation is often used to describe particle interaction, but usually inside numerical methods. The harmonic balance and Fourier series methods are used to quickly solve the particle damper equations. A Poincaré map is also used to observe the behavior of the analytical systems.

One approach to model particle beds is to use a computational fluid dynamics (CFD) toolbox. For example, a widely available software suite which allows the modeling of particles is OpenFOAM.[4] Some published research, such as Leitz et al. [35] rely on the software package's ability to track particles. However, the approach of Leitz et al. [35] does not implement a contact model within OpenFOAM. The impact calculation is instead performed in Abaqus and the equations are not available in the article. Another simulation done by Dissanayake et al. [36] uses OpenFOAM for modeling particles in a flow, but no information is given on the choice of collision model. Nevertheless, the choice of a suitable collision model is fundamental for modeling the dynamics of particle dampers.

[1] this term is not used consistently in the literature and often the exact definition is not given, so it has to be handled with care.
[2] this term is not used consistently in the literature and often the exact definition is not given, so it has to be handled with care.
[3] variations of this definition also exist.
[4] http://openfoam.org.

According to the online[5] documentation and user/contributed information for the different distributions of OpenFOAM, its particle modeling features are: particle tracking algorithm which works with moving meshes; particle injection; particle drag in the containing medium. Two trajectory models are implemented in this particle simulation approach of OpenFOAM and they are both based on the same particle collision model by O'Rourke et al. [37] which is based on the probability of a particle being in a specific zone. This latter method is an extension of the multiphase particle-in-cell (MP-PIC) method. Although CFD can also be used to model the fluid between the particles, such an approach may be excessively laborious for the resulting increase of accuracy. Resources may be better used to properly tune a simulation of particles only.

The methods of regression analysis, restoring force surface, power input, and neural networks were also used for particle damper simulation [38]. While they can bring some insight on the particle damper behavior, these models are usually no longer valid outside of their experimental boundaries [39].

Consequently, numerical solutions for particle dampers usually rely on implementations of the discrete element method (DEM[6]) to solve the analytical formulations mentioned earlier. It is common to see approaches that reduce a multiple DoF system into a simpler equivalent system. The equivalent system is usually damped and elastically supported and has a single or a few DoFs. Dashpots and springs of these reduced models can take various forms. They can be assumed to either: always be in contact; activate according to the system's position; have non-standard physical properties, such as nonlinear force-displacement and force-velocity curves; or, respond according to a rheological model. These equivalent systems are usually obtained either from analytical derivations or from experimental data. Modeling friction between the particles is often reported as a challenge by the authors and is sometimes neglected due to the limited influence of friction in particular configurations.

3.1. Particle damping analytical methods

An attempt to provide analytical solutions from the literature is provided by this section. However, as the reader will notice, most of the proposed approaches require numerical methods to be solved. This is a consequence of the highly nonlinear behavior of particle dampers. Numerical solutions will be treated more in detail in the subsequent section.

Olędzki et al. [11] use a rheological model where a metal, that is considered non-deformable, is damped when in contact with a plastic. The model is described by the following equation, where the parameters a, b, c, and d are calibrated with experimental data from the plastic materials

$$m\ddot{x} + ax|x^b| + c\dot{x}|\dot{x}^d| = 0 \tag{1}$$

Ibrahim [3] reports many uses of modeling the impact of a particle with a wall using an equivalent force based on distance with the wall. He also reports the use of a coordinate transformation method which analyzes the impact model using position-based coordinates instead of time-based ones. He reports that damping functions are also based on the penetration depth of the impacting bodies, with quadratic or cubic relationships. This last method is referred to as the Hertzian contact. Ibrahim [3] also reports that different analytical methods were used for both harmonically excited and decaying impact damper responses and that optimal relations between particle clearance, coefficient of restitution (CoR), and vibration amplitude exist. Brogliato [40] makes the distinction between the vibroimpact mechanics, which usually focus on one or few masses, and billiards, which refer to multi-particle systems. When used for damping purposes, these two types of systems are often referred to as impact dampers and particle dampers, respectively. Ibrahim [3] rather focuses on the former type of contact. Fang et al. [41] instead relies on the Hilbert Transform to obtain relationships between the different parameters of the particle damper and its efficiency. Bryce L. Fowler [18] use a method similar to the DEM which explicitly solves the motion of the individual particles by assuming that they only interact with their immediate neighbors during a timestep chosen sufficiently small to allow this assumption. This, however, contradicts the wave phenomena reported by Brogliato [42]. As many other models reported, the method of Bryce L. Fowler [18] uses a variant of the Hertz method to measure the force between colliding bodies. For oblique impacts, they measure the forces using Coulomb's law. They mention that some authors use an additional viscous friction force of which the purpose is to limit strong oscillations in the measured forces. In their calculation for the response of a damped beam they, as many other authors, represent the beam using an equivalent single DoF mass-spring-dashpot system. Saeki [43] considers the individual particle's contributions to a complete horizontally vibrating system made of multiple units of particles. To simplify, or rather speedup, the analysis they assumed that each unit behaves in the same manner and they thus reduce the analysis to the number of particles contained in a single container. They calculate the contact forces using Hertzian theory and the tangential forces using Coulomb's law of friction. The spring constant of the Hertzian contact law uses Poisson's ratio and the modulus of elasticity to link deformations to displacements. They solve the system by integration over time.

Szmidt and Zalewski [44] model the particular damper vacuum sealed beam, a VPP, as a combination of Euler-Bernouli beam theory and a Kelvin-Voigt material. They also neglect gravity forces as their beam's long edge is placed vertically.

Park and Palumbo [45] are mostly interested into mitigation of vibration-induced sound. Their model thus considers both airborne and frame wave propagation. They conduct their analysis of the beam using the classical beam formulation for their

[5] https://cfd.direct/openfoam/free-software/barycentric-tracking/https://openfoam.org/release/2-3-0/dpm/https://www.cfd-online.com/Forums/openfoam-announcements-openfoam-foundation/190919-openfoam-5-0-released.html https://www.cfd-online.com/Forums/openfoam-solving/134605-particle-collision-model-mppicfoam.html.

[6] DEM is also known as the Distinct Element Method.

main beam where an additional loading term is obtained from a wave analysis of the particle-induced pressure on the frame. They solve that beam equation using the Rayleigh-Ritz method and mention shear damping of inner honeycomb panels could be considered by using the Timoshenko beam. Their equations are solved by a Newton-Raphson integration and correlate well with their experimentally obtained transfer functions of the beam with and without inner particles.

Lu et al. [12] provide a method to optimize the design of a tuned particle damper. It starts with the determination of the required material density, which should be as low as feasible. The mass of the cavity should also be constrained to a range, and kept as small as possible with respect to the total particle mass. The fill ratio can then be imposed to be between 20% and 90%. The frequency of the structure, for civil engineering applications, should be between 0.5 Hz and 3 Hz. Their analytical equations can then be used along with a selected optimal clearance to obtain a predicted structure displacement. However, these equations are to be solved numerically. An iterative procedure can then be conducted to identify the best parameters from the previous steps using the later analytical equations. Finally, the optimal parameter of particle mass leads to the number of particles, and the optimal number of layers leads to the related cavity dimensions.

The model of Du and Wang [46] is mostly analytical, but is nonetheless resolved through numerical integration. They represent their combined impact and particle damper consisting of a large mass and a granular material by an equivalent two DoF viscoelastic system. They model the impact of the large mass and the main structure, which are both covered by the fine, powder, granular material as a particle to particle impact. They, however, change the particle's mass and velocity to be those of the damping mass and main structure.

3.2. Particle damping numerical methods

Yokomichi et al. [47] are able to model a system with multiple particles using an equivalent single DoF system. They also consider that a complete bed of particles can be represented by an equivalent single mass body without friction that collides plastically.

Ibrahim [3] mentions that the multibody dynamics can and have been used to solve impact damping. He, however, adds that such a formulation is complicated and that the presence of friction makes the problem difficult because of reverse sliding and sticking. He also mentions the use of partial differential equations to solve continuous systems, such as beams, subjected to impact damping. Brogliato [42] underlines that the multibody formulations used for single and multiple impacts are different. For the former, only one collision occurs at a time in the system while in the latter multiple collisions can occur simultaneously. With multiple simultaneous collisions, a wave propagates through the contacting bodies and lengthens the duration of the contact. This is at least the case for systems of aligned particles. Some of the simulation methods [48] are developed for real-time simulation and gaming engines. Iglberger and Rüde [48] and Iglberger and Rüde [49] thus introduce a physics engine which allows multibody simulation of particle collisions while focusing on obtaining behaviors which respect the laws of material science. Their engine provides good scalability through message-parsing interface (MPI) parallelization. From Dassault, Elmqvist et al. [50] also present another multibody-based approach focusing on correct physical representation of the particle collisions. They rely on a DEM. The DEM formulation was first presented by Cundall and Strack [51] and consists of modeling each particle individually using a contact model that causes viscoelastic forces to be exchanged between the particles. Ehrgott et al. [52] use an axisymmetric finite element method (FEM) to study the impact of particle dampers on a turbine high pressure seal of a space shuttle. They ensure the natural frequency of the damped seal remains unchanged by the addition of the particle damper by using a material for the pellets which has a low modulus of elasticity. They also incorporate their test fixture into the FEM analysis. Their approach models the pellets using their strain energy and they conclude that the method shows limitations due to the underestimation, for certain modes, of the damping they obtained experimentally. Multi-DoF (MDoF) models use spring and damper analogy to simulate particle-particle and particle-wall collisions.

Wong et al. [19] mention that obtaining particle-level detail on the workings of the particle damper seems to be the only way to properly predict its damping efficiency. They thus state that DEM, used with a soft sphere model, is a viable solution method. The soft sphere model, as opposed to the hard sphere model, implements more than just the coefficient of restitution and thus considers friction and damping between the particles. They also provide the equation to obtain the critical, thus maximum recommended, timestep. They use a timestep equal to 80% the critical one, thus using a safety factor.

Saeki [53] uses DEM to simulate the damping action of a granular bed and finds good correlation with the experiments. DEMs are commonly used to simulate excited particle beds and a thorough introduction to these methods is given by Matuttis and Chen [54]. Two DEM implementations are used by Kwarta and Negrut [55] to model the interaction between particles of different shapes and properties.

Lu et al. [6] mention that most DEM applications are concerned mostly with the particles and that the containers are usually fixed or have an imposed motion. In the case of the particle damper, the main structure responds to the influence of the particle damper. They thus warn that traditional DEM must be adapted to allow interaction with the containing cavity and structure. In their case, the modification consists of adding the equations of motion of their main structure to the DEM formulation. They nonetheless bring to attention the need for DEM models of particle dampers because many applications are concerned with more than a single vibration mode and frequency and thus cannot be properly modeled by single DoF equivalent systems. They solve their particle-system interaction problem using a strongly coupled method where they iterate at each timestep until particle-induced forces and structure displacement converge.

Lu et al. [6] proceed to a first validation by inspecting the response of a single particle and comparing it to the analytical solution. Then they reproduce the experimental results of motion against frequency of a single DoF structure with both a single

unit and then with a multi-unit particle damper published by another author. Finally, they conduct an experimental campaign where they excite a scaled 3-story building using the motion time histories of four earthquake. The building is equipped with a particle damper on the roof. Their simulations use a timestep of 1×10^{-4} and are able to adequately reproduce the behavior of displacement and acceleration measured at the different floors of the building.

The in-house DEM implementation of Wang et al. [56] has a contact law based on the Hertz formulation and uses Coulomb friction forces. They use a link-cell method with two short lists for contact detection. This significantly reduces the computation time when compared to the traditional all-pair with one long list contact detection method. They report remarkable agreement with their experimental data, and being able to reproduce a dip in the damping-acceleration plot that prior authors were not able to model. They use stainless steel spheres of 1 mm diameter. Their work highlights the advantage of DEM over empirical formulations because it allows them to closely analyze the internal mechanisms that cause damping. For example, they are able to analyze the proportions of dissipation caused by particle-particle and particle-wall interaction and further separate these categories into losses due to friction and inelastic collision.

Duan and Chen [57] use a DEM implementation with a velocity-dependent coefficient of restitution. Their equation, taken from the literature, gives a coefficient which reduces with velocity. They justify their choice by stating that the coefficient of restitution has an important impact on energy dissipation. They impose the maximum particle tangential force to be determined by the Coulomb friction while lower values are dictated by a viscoelastic law. They demonstrate that their model with the velocity-dependent coefficient of restitution is better able to reproduce their experimental results. However, it is not clear whether, to compare velocity-dependent and constant coefficients, they retuned the model with the constant coefficient for their empirical parameter. Different results could emerge if they simply substituted the coefficient inside their model which was already empirically tuned. It is also not clear whether they tried different constant values of the coefficient of restitution or what criteria was used to choose the constant value of 0.95.

Although the particles of their experiments have irregular shapes, Xu et al. [7] assume them to be spheres for their numerical approach. They mention that other researchers have demonstrated that this assumption is valid for particles size below a fifth of the cavity's size. For their longitudinal beam particle damper, they use a reduced particle model. It represents the impacts inside the particle bed as if the bed was made of a single layer of larger impacting particles of the same total mass vibrating only in the longitudinal direction. As such, they rely on an adapted Hertz contact model. Finally, they numerically solve the equations of Euler-Bernouli beam theory with additional forces provided by the impact and shear friction of the damper and the beam's internal damping. They use an explicit method and a 20 μs timestep.

For their numerical simulations of a particle damped gear, Xiao et al. [39] use DEM with a 10^{-4} s timestep. They mention that it is a method which assumes constant velocity and acceleration over a timestep. They import the multibody dynamic solution of the gear angular velocity and acceleration of the gears into the DEM solution.

Klinge [58] conducted preliminary tests using DEM to simulate a particle damper. The particle damper is a cavity with 6 mm steel spheres modeled as having the Young's modulus and Poisson ratio of limestone, to reduce the computational time by roughly two orders of magnitude. He then switched to the Abaqus DEM module, which can be combined with the FEM simulations. He then feeds the model to an optimization procedure ran inside the Dakota open source optimization framework. He uses real numbers for the optimization and then rounds appropriately for the parameters that request integers. He limits the study to spherical particles of the same material. He also checks that the numerical solver is able to converge at the vertices of the optimization search domain. He finds the Parallel Direct Search algorithm to be the most efficient at finding the optimal damper configuration. His simulations take roughly 1000 times the realtime to solve. This number varies with the input parameters. He concludes that stiffer materials solve faster by having fewer simultaneous contacts during the simulation, but this contradicts the fact that using the modulus of elasticity of limestone made the simulations 100 times faster than when using that of steel.

Chodkiewicz et al. [59] further develop the DEM method to allow modeling of Vacuum Packed Particles. The VPP is a particle damper where the cavity is replaced by a foil, or envelope, which is maintained under partial, and controlled, vacuum. This allows to actively modify the particle arrangement inside the damper and consequently the damping response. Their modeled cavity, here being the whole structure, reacts to external pressure caused by the vacuum. This is modeled in the DEM using an external cover represented by spheres of smaller thicknesses than the actual cover. They do so to ensure proper discretization of the foil. They apply the external pressure as a force to selected particles which constitute the external envelope. That force is calculated from the pressure and a particle-dependent area vector. Their paper gives the geometries of the particles and damper along with the Young modulus and Poisson ratios necessary for the DEM. They validate their method through qualitative comparison with hysteresis loops of displacement-force coming from prior experimental data.

Wang et al. [9] couple discrete element and finite element methods where the DEM captures the particle contact and the FEM the response of the structure. They assume the DEM timestep to be small enough to prevent issues emerging from new contacts and transmission of forces to other particles. This is also stated by Lu et al. [6] who mention that the timestep must be small enough to prevent disturbances on one particle to propagate any further than its immediate neighbors. Wang et al. [9] define stiffness and damping coefficients that are used by the spring and dashpots normal force models of particle-particle and particle-wall contacts. The tangential contact forces are modeled by Coulomb friction. To accelerate their numerical study, they focus the analysis in narrow frequency bands near the natural frequencies of the structure. They also assume that all particles are spheres with the same diameter. Their model allows them to identify the optimal particle density, mass ratios, and cavity depth. Their experimental results then reproduce the trends observed by their numerical model.

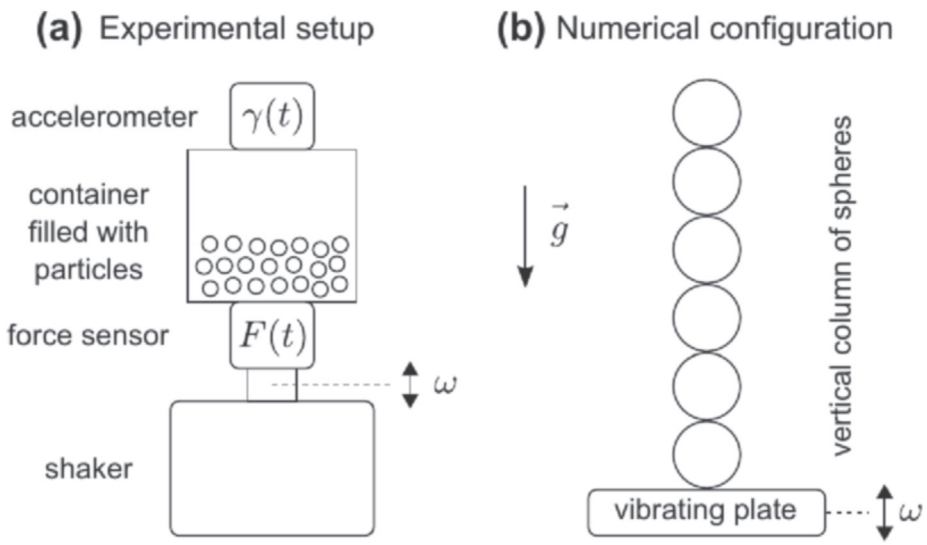

Fig. 2. Experiments (a) and simulations (b) of Masmoudi et al. [60]. Reprinted with permission from Springer Nature.

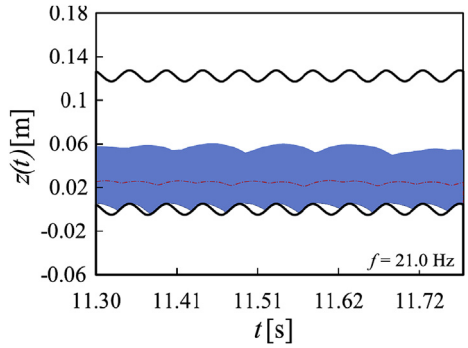

Fig. 3. Gas behavior from the simulations of Sánchez et al. [21]. Reprinted with permission from Elsevier.

Masmoudi et al. [60] use DEM to create a simplified representation of their experimental particle damper test bed. The simplification consists in representing the cavity and particles as a single column of superimposed particles. Both their experimental and DEM configurations are shown in Fig. 2. Their timestep is determined by ensuring it remains well below both the contact duration and time a wave takes to cross the particle. They use a wave speed value which is function of Young's modulus and density.

Sánchez et al. [10], Sánchez and Carlevaro [61], Sánchez et al. [21], and Sánchez and Pugnaloni [62] use their in-house DEM implementation to model particle dampers. They give the coefficients of restitution and friction for both the walls and the particles used by their simulations. Although their results match the generally observed trends, they provide little comparison with experiments.

The DEM implementation of Sánchez and Pugnaloni [62] uses quaternions to represent orientations. Their normal interaction force between the particles is calculated using the Hertz-Kuwabara-Kono model. Their tangential forces instead come from the minimum value between the Coulomb law of friction or the shear damping force. They give the particle parameters necessary to run their DEM. They conclude that their algorithm produces results that qualitatively concord with experimental findings of other authors.

In another work, Sánchez et al. [21] provide a justification to use a single lumped mass impact damper equivalent system. They demonstrate that in most cases, this simple equivalent system provides the same damping properties. They also present an innovative plotting method which allows to visualize the time-marching response of both the structure and the particle bed together on one plot. An example is shown in Figs. 3 and 4, which also highlight the gas and lumped mass behaviors of the particle bed, respectively. The gas behavior, in this case, occurs at frequencies beyond 18 Hz.

Coetzee [63] also mentions that most DEM approaches rely on spherical particles to be computationally efficient. A popular approach to model different shapes is to rely on clumps, which are the agglomeration of more spheres into a single particle. Clumps have the advantage of still relying on the efficient contact-detection algorithms designed for spheres.

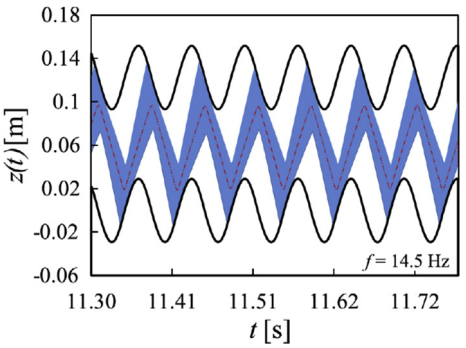

Fig. 4. Lumped mass behavior from the simulations of Sánchez et al. [21]. Reprinted with permission from Elsevier.

Coetzee [63] further mentions that reducing the contact stiffness by a factor of up to 1000 is a common method that allows reducing computation time. It can reduce the simulation time by at least one order of magnitude, but care has to be taken not to exceed a reasonable particle overlap, and still properly reproduce the important characteristics of the experiment.

3.3. Non-DEM particle damper identification

Bajkowski et al. [64] proceed to parameter identification of their non-DEM particle damper model through an optimization process. Their identification approach is similar to the least squares method and is applied to the displacement signal taken at each timestep for the first 30 s of simulation. They add that this method works well because they have models based only on equivalent stiffness and viscous damping. The optimization would be impractical if nonlinear friction was introduced.

For a particle damper, Zalewski and Chodkiewicz [65] use a 6-parameter model which also includes the effect of wear as a modifier of the viscous damping coefficient. The wear modifier is a function of the total damper displacement and experimentally determined coefficients. Their model also has a Coulomb friction force. They use an evolutionary optimization algorithm with a population of 40 and 200 generations to obtain the parameters. The algorithm is used to minimize the error between the experimental and numerical force-displacement hysteresis loops of the damper.

For their previously covered approach, Michon et al. [8] relies on both manual interpretation and on the least mean square method to identify the parameters which characterize their particle damper. To do so, they use force-displacement curves other experimental data.

4. The discrete element method for particle dampers

The previous section drew attention to the predominance of DEM when simulating particle dampers. Actually, the most popular method to simulate agglomerations of dry macroscopic particles is DEM. Furthermore, the need to simulate the particle bed by individually modeling each particle is reinforced by the following peculiarities [66]: 1) the aspects of the excitation forces will influence whether the particle bed behaves as a fluid, as a solid, or as a gas; and 2) granular material does not mix homogeneously as fluids and particles usually aggregate according to their sizes.

Most published DEM simulations model between 100 and 1 million particles [67]. DEM also is often combined with computational fluid dynamics or finite element methods [63]. Such combinations allow to model the interaction between particles and fluids or deformable elements. The deformable elements can also be the particles themselves. These coupled methods are often classified as extended discrete element methods (XDEM), but this document relies on the term DEM for both coupled and uncoupled methods.

Consequently, some aspects that must be taken into consideration to perform DEM simulations are discussed. This section thus covers the detection of contacts in 4.1; normal contact force models in 4.2; tangential and friction force models in 4.3; the coefficients of friction and restitution in 4.4; numerical aspects in 4.5; and, the choice of software toolboxes in 4.6. Focus is mostly given to cases where particle dampers are involved.

4.1. Contact detection

Contact detection, also known as collision detection, contact determination, and interference detection is an important aspect of a DEM implementation. It can consume a considerable amount of computer resources [56,68,69], especially when non-spherical and complicated particle shapes are used. The most resource demanding collision detection is when particles of non-convex shapes are involved [54]. Usually, detection is done using a two-phase procedure. The first is called the broad phase and identifies every pair of particles that may come into contact at the current timestep. The narrow phase then performs a

more accurate verification and identifies times and positions at which collisions occur. Doing this two-step procedure allows to limit the amount of accurate verification done by the algorithm.

Particle shapes for numerical simulations can be defined by polygons, constructive solid geometry, implicit functions, and parametric surfaces [69]. Methods using optimization can be used to solve for collision detection of complicated shapes. Hierarchical representation of objects can be used with methods of Bounding Volume Hierarchies (BVH) [70]. They consist of gradually refining the shape of the particle using bounding boxes which can have cubic, spherical, or other analytic shapes. They are the most common methods for collision detection [71] and include the Axis-Aligned (AABB) and Oriented Bounding Boxes (OBB). The former uses boxes which are aligned with the global coordinate system while for the latter they align with the object. AABB is simpler to use while OBB is faster because it follows the object if a rotation occurs. A series of such BVH for different shapes exist [71,72]. However, here and for particle dampers in general, most simulations use spherical particles. Thus, simpler analytic contact detection algorithms may be used.

Wang et al. [56] find considerable improvements by a proper choice of broad-phase contact detection algorithm. Their simulation is made of equal-dimension spheres of a uniform material. They report that the solution of the DEM using the Link-Cell broad phase contact detection algorithm used with two short lists for contact storage was seen to be up to twice as fast as an all-pair method with a single list. The Link-Cell is a method that decomposes the particle domain's two-dimensional projection into a series of cells created by subdivision of the resulting projected area [73]. By choosing the edge length of the cells adequately, they are able to exclude collision between particles that are not either in the same cell or in neighbor cells. The Verlet table consists of maintaining a list of the particles that are within a given distance of each other and that could thus collide in the upcoming timesteps [73].

As a warning, Lin and Gottschalk [69] mention that rating the efficiency of different collision detection algorithms is not feasible. In reality, they each have specific applications where they are very efficient and others where they are slow. Nevertheless, they attempt to rate the efficiency of the algorithms based on the relationship between the number of operations required to resolve the contacts inside a simulation with n bodies. Under that interpretation, a naive implementation would require n^2 operations [68].

Nevertheless, Rousset et al. [68] compare 10 broad-phase collision detection algorithms with the purpose of identifying the fastest ones. They test a 3D particle bed of variable radii spherical particles with n going from 100 to 1 million. Their tests are run on a single computer core and they identify memory and time consumption for the solutions. They conclude that the LooseOctree, Octree and Sort&Sweep, Bruteforce, Hierarchical Grid, and Kd-tree algorithm are too slow for practical uses of their simulation because they require approximately 1 s to execute with 10,000 particles. On the other hand, they identify the Bullet and CGAL algorithms as fast. They find that Sweep&Prune is the fastest when few particles are involved and that Simple Grid is the fastest when many particles are involved. For the fast algorithms, the execution time for 1 million particles varies between 3 s and 60 s.

The simulation of Dinas and Banon [71] instead shows the importance of choosing the bounding volume adequately for the specific application. They find that by changing the complexity of the particle shape, the faster contact detection algorithms can become the slower ones, and vice-versa.

Stating that the contact detection algorithm requires considerable simulation time, Lu et al. [6] chose to rely on the no binary search (NBS) approach. They obtain a search time proportional to n while the time for a binary search algorithm would scale with $n\ln(n)$. They state that the algorithm's solution time scales linearly to the number of particles and is most efficient for particles of similar sizes. This corresponds to their particle damper which is filled with identical spheres.

Other methods for contact detection include geometric and algebraic formulations, partitioning of space, and optimization [69]. Finally, the review of Lin and Gottschalk [69] provides a starting point for terms and concepts associated with contact detection of more complex shapes.

4.2. Normal contact forces

The choice of a contact model for a DEM simulation is arguably the most influential aspect on the results because it computes all non-inertial internal forces of the system. For these forces, a variety of elastic and viscous models in both normal and tangential directions are available. A brief overview of the commonly used models is given in this subsection for normal contact forces and the next subsection for shearing, or tangential, contact forces. Although not covered, the position of application of the contact forces and the calculation of the penetration depth which is used to compute these forces are other facets to consider for DEM codes. The contact area is another key parameter [74] for which the reader is referred to the literature. For particle impacts, energy dissipation regimes can be based on formulations such as hysteresis, plasticity, elastoplasticity, waves, or viscosity [74].

In their general paper on DEM contacts, Elmqvist et al. [50] use a generalization of the Hertz contact model because they treat non-spherical particles. Their normal force is defined as proportional to $\sqrt{Vd}$ where V is the volume of overlap and d is the penetration depth. They mention that damping can be added.

To reproduce material science theory, impacting bodies should initially deform elastically and then plastically. The original DEM implementation [51] relies on a linear, Hooke, normal elastic force to which a linear viscous force is added. This modeling approach is still valid today, however, diverse adaptations are also seen in the literature. Effectively, for particle dampers, the

elastic portion is usually modeled by a Hooke [6,9,19,75] or a Hertz [5,39,53,56–58,60,62,76,77] contact force. The Hertz contact law is the most popular choice. It is described by Timoshenko [78] and was originally presented by Hertz [79]. On the other hand, the plastic portion of the contact is often modeled by a linear [5,6,9,19,39,57,75] viscous force. Other plastic portions are either based on the fourth root of the displacement multiplied by the velocity [56,60,80] or on the proposal of Kuwabara-Kono [62]. To summarize, given that v is the normal contact velocity, the proportionality of the different contact force models are: $\propto d$ for Hooke or linear; $\propto d^{3/2}$ for Hertz; $\propto v\sqrt{d}$ for Kuwabara-Kono; and $\propto vd^{1/4}$ for another alternative.

By will of the multiplying constants, the resulting viscoelastic force is often an indirect function of the coefficient of restitution or Young's modulus and Poisson's ratio. For example, the Hertzian contact model defines the spring constant as

$$k_n = \frac{\sqrt{2r}}{3}\frac{E}{1-\nu^2} \tag{2}$$

where r is the radius of the spheres, E is the modulus of elasticity, and ν is Poisson's ratio. Equation (2) applies for two spheres having the same radii and material, as it is a contraction of the version for different spheres. Wong et al. [19] calculate the stiffness constant for their linear contact law by imposing that when the yield condition is reached the stored energy is the same that would have been stored with a Hertzian contact. As for dissipation, the damping coefficients have diverse definitions which can be based on the stiffness coefficient, mass, and coefficient of restitution of the particles [5,39]. Alternatively, Wong et al. [19] obtain the critical damping ratio from the CoR and then from this ratio the damping constant. A different, common choice is to use the damping factor as a calibration parameter of the simulation [74]. Finally, there are diverse methods used to compute the spring, damping, and other constants used in the contact force models. A comparison [77] between the force to deformation relationship for a sphere modeled both with Hertz contact theory and with finite element analysis indicates that the Hertz model remains valid for small deformations. Actually, this corresponds to the assumptions of the Hertz model.

4.3. Tangential contact forces

The Hertz contact model only deals with force exchanges in the normal direction. Yet, in a DEM simulation, many oblique contacts can occur and they thus need to be considered. A series of variations exist on the choices of treatments made by the different authors. The most popular historical implementation comes from Mindlin [81]. Thus, often the chosen contact model is referred to as the Hertz-Mindlin model. In that model, the normal force and the radius of the contacting surface are calculated from the Hertz formulae. Accordingly, this subsection presents a few shearing force models from the particle damper community.

Coulomb-type tangential friction models are very common when modeling particle dampers [6,9,13,18,43,56,62,82,83]. It works well for the long-lasting sliding contacts which are dominant in particle dampers [6]. For general DEM of regular packings, partial slip has a subtle and non-dominant influence [67]. Care must, however, be taken when using the Coulomb friction model as it can induce oscillations at small relative displacement.

Some implementations [13,56] use pure Coulomb friction for their tangential contact forces. Others use the Coulomb friction force as the maximum value the particle tangential contact forces calculated from an elastic or elastoplastic displacement laws can take [57,62,84]. This is the case of the Hertz-Mindlin tangential forces [81]. Others rely on Coulomb-type friction forces in a more elaborate manner. For example, He et al. [85] use a tangent contact force model proportional to the normal load multiplied by the displacement accumulated during the contact period. They cap it to a maximum value and also add capillary and particle bonding forces.

No report of using a dynamic, state-dependent, friction model of the LuGre-type [83,86] is seen in the literature. Many implementations do contain both normal and tangential elastic and viscous force laws, but they are usually applied simultaneously. Balevičius and Mróz [87] develop a friction model for contacting spheres that differentiate between slipping, at low driving forces, and sliding zones, at large forces. A mention of the stick-slip phenomenon is also made by Hayakawa [88], but the authors focus on the behavior of the particle bed. Thus, they model tangential friction at the particle level using an elastic force. One explanation for the absence of friction model of the LuGre type for the contact is that they are limited to applications with unidimensional displacements. Effectively, in particle simulations, the relative displacements of the particle's contacting displacement are bidimensional and can involve relative twist as well.

Syed et al. [89] instead use rolling friction of the particles to compensate for the use of purely spherical particles when modeling non-spherical particles. This method is also proposed by Wensrich and Katterfeld [90] who warn about strong discrepancies in the results it yields. They also indicate that one issue of the method is that rolling friction always opposes rotation of the spheres while the irregularities of the shape of a particle do not always do so. That approach is also severely criticized by Matuttis and Chen [54] for similar reasons. To provide increased accuracy, Syed et al. [89] develop a coupled rolling and sliding friction coefficient based on the energy balance of the particles. They also report use of Coulomb for purely tangential friction. Nevertheless, Wensrich and Katterfeld [90] report that the rolling friction method is commonly used in the literature and that different friction-like models are used for the purpose. The most common ones compute the rolling resistance force as proportional to a) the normal contact force; b) the normal contact force and relative velocity; c) the viscoelastic resistance applied to the displacement since the last timestep; or d) relative angular velocities.

For soft spherical particles, Holmes et al. [91] develop a friction model for not only rolling and shearing, but also bending and twisting relative motions. They do so to replace the rolling component between the contacting particles. Their shear friction force is from a viscoelastic law and is based on the relative velocity between the particles and the contact overlap.

Sohn et al. [92] also use a viscoelastic tangential contact force model and study the impact of different friction coefficients on the results. In their viscoelastic model, the Coulomb friction law is imposed as the upper limit that the viscoelastic tangential contact force can take.

This concludes the subsections on contact forces in DEM, but they are not exhaustive by themselves. Effectively, not only can DEM contact forces be both elastic and viscous and be applied in the tangential and normal directions, but they can also include pivoting[7] and rolling; can be shape-dependent; can use different stiffnesses for approach and departure; and more. Further discussion on contact models for DEM can be found in Horabik and Molenda [74] and Machado et al. [93]. The reader should nevertheless keep in mind that the more complex nonlinear contact models such as the Hertz and Mindlin formulations are not always more precise than the simpler linear models [6].

4.4. Coefficients of friction and restitution

In most cases, the coefficient of friction refers to Coulomb's Law of Friction:

$$F_f \leq \mu F_n \tag{3}$$

where F_f is the resulting friction force, μ is the coefficient of friction, and F_n is the normal contact force. Various adaptation of the law can be seen in the literature.

The coefficient of restitution is a measure of the absorption of energy during an impact. It is defined as

$$e = \frac{v_i}{v_f} \tag{4}$$

where v_i and v_f are the relative velocities of the colliding particles before and after impact, respectively. A totally elastic impact yields a e of 1 while a totally plastic impact yields a null e.

Obtaining the right values for μ and e can be a time-consuming task. When the particles are perfect spheres, these coefficients can be obtained from individual testing of particles. Nevertheless, substantial differences can arise between the coefficients measured individually and those obtained by bulk calibrating a DEM model. For example, using a particle-particle friction coefficient that depends on the average normal load can improve the accuracy of shear tests conducted with steel spheres [94]. Additionally, obtaining accurate values for these two coefficients may not be necessary. Effectively, some authors find very little variation [19,21,56,77] of the damping efficiency when changing the restitution and friction coefficients in simulations of optimized particle dampers. This subsection thus attempts to resume the literature relating to these coefficients when they are used in particle damper DEM simulations.

Different authors prefer a coefficient of restitution, e, which varies with speed [57,74,95]. Alternatively, others rely e on values which are considerably higher than the experimentally obtained values. The experimental data of McNamara and Falcon [95] for steel spheres gives a coefficient of restitution which goes from $e = 0.95$ at $v_i = 0.1$ m/s to $e = 0.65$ at $v_i = 1$ m/s. Their numerical simulation of a particle bed vibrating on an excited piston confirms the necessity for a variable coefficient of restitution. They also define a tangential e which is the ratio of the tangential velocities before and after impact and has a range of $[-1, 1]$, if no energy is created by the impact. Wong et al. [19] instead mentions that the e is not dependent on impact velocity but rather on the compressive work done on the particle.

The simulations of Lu et al. [13] show that the e's influence on the damping efficiency also depends on other geometric parameters. For example, a smaller e will provide better damping for small container sizes while the opposite is true for large containers. They also note the counterintuitive behavior that an increase in the sliding friction coefficient sometimes reduces the damping efficiency. They explain this by the reduced momentum exchange caused by having fewer collisions in turn caused by the smaller particle velocities due to the increased friction. This explanation is complemented by Xiao et al. [38] who simulate the damping of a gear with particles and mention that at higher e the number of collisions increases because each one has a shorter duration. As expected, the effect does not cover all operating conditions and thus for high gear rotating speeds, smaller e's provide better damping. Lu et al. [96] also find that for single axis excitation the influence of the e is limited. They find that its influence becomes more important as the size of the cavity in the direction of excitation increases. Correspondingly, smaller e will cause higher sensitivity to increases in container size.

On the other hand, Sánchez et al. [21], who also use a tangential coefficient of restitution, numerically find that both friction and the coefficient of restitution have a negligible impact on the response of the particle damper. This is e related to their universal response for a particle damper. Their explanation is that the resulting behavior occurs because the overall impact of the particle cloud is an inelastic collapse. Thus, the resulting overall coefficient of restitution is null and remains as such while e's and μ's for individual particles are varied because. Effectively, when many particles are involved, almost totally elastic e's and μ's still dissipate enough energy to result into an inelastic particle cloud collision with the cavity walls. This behavior is not observed in other regimes such as the gas-like regime where the cavity ceiling would be for example higher. In that latter regime μ and e do impact the total energy dissipated by the damper. Nevertheless, particle dampers operating in their optimal range can be modeled as a cavity with a single particle having $e = 0$ and the mass as the particle cloud [21,47]. Wang et al. [56] also finds negligible influence from e. This also applies to their mixed horizontal-vertical excitation. Moreover, they

[7] also referred to as twisting.

also find little influence of μ and its increase actually decreases the total damping. Also, DEM simulations showed that for given excitation amplitudes and frequencies the power dissipation for both $e = 0.3$ and $e = 0.65$ are almost equal, when all other parameters remain unchanged [19]. The change rather appears in the amount of energy dissipated by each of these two dissipation mechanisms, namely friction and impact. The work of Darabi [77] agrees with these observations by finding that, although friction is a major mechanism of energy dissipation in particle dampers, changes in the value of its coefficient do not significantly affect the power dissipated. This is once again explained by the changes in the relative contributions from the different dissipation mechanisms. They often compensate each other and lead to an unchanged total energy dissipation.

4.5. Numerical aspects

Any DEM implementation has to rely on numerical methods to time-integrate the equations. This involves a series of algorithms that vary depending on the code used and the choices made by the users. A quick overview is given here.

The choice of minimum timestep can be done using the Rayleigh timestep [39]. The Rayleigh timestep is a function of geometric and material properties of the particles. Another method is to ensure that at least 6 timesteps occur over a contact cycle [5], thus containing both compression and rejection phases of the impact. Lu et al. [6] instead states that the timestep should be chosen small enough to ensure that the disturbance caused by a particle does not affect any other particle beyond its immediate neighbors. Consequently, they chose a timestep of 1×10^{-4}. Darabi [77] uses a critical timestep which is the inverse of the highest natural frequency in the system. It is determined by computing both translational and rotational frequencies and multiplying the minimum by a safety factor of 0.8. Sánchez et al. [10] use 0.005 s for triangles and hexagons of circumscribed radii varying between circa 1 mm and 20 mm while Sánchez and Pugnaloni [62] use a timestep of 8.75×10^{-8} s for particles of 3 mm radii. A similar timestep is used by Fleischmann [97] as calculated using the method described by Darabi [77]. Also for a particle damper, Pourtavakoli et al. [98] use a timestep of 10^{-6} s which is 20 times the collision time. They calculate the latter as a function of the impact velocity, an elastic parameter, and the effective mass.

The integration of the equations is often done using a central finite difference scheme [5,75,77,97]. Some particle damper solutions are also obtained with a fourth order Runge-Kutta [13] or the velocity-Verlet [61,62] integration algorithm. The later estimates both position and velocity at the next timestep using the velocity at the current timestep. Alternatively, the original integration method of [51] uses an explicit scheme. Its simplified outline is as follows: 1) calculate displacements at time t_{i+1} as $v_i \Delta t$ where Δt is the timestep and v_i is the particle velocity; 2) sum all forces acting on the particle using the new positions obtained from the displacements of step (1); 3) use these forces with Newton's second law to obtain the particle accelerations at time t_{i+1} which remain constant until time t_{i+2} and thus serve as input to step (1) where the cycle repeats itself for a new timestep.

4.6. Software implementations

The original DEM code was called BALL and is described in Ref. [51]. The years immediately after its publication saw little or no other publications on the subject. Then, around the 1990s the number of publications increased steadily to reach today's roughly thousand annual publications [67] for a cumulative total of circa 10,000 citations. Consequently, a series of similar codes were developed. A few examples are Aston DEM; Abaqus; ELLIPSE3D; TRUBAL, modified TRUBAL; LAMMPS; modified LAMMPS; LIGGGHTS; LS-DYNA; PFC; Oval; YADE; EDEM; DEMeter++; DEMMAT; Mercury-DPM; and, Chrono. Other authors present their own formulations and implementations [13,66,91,92]. This section thus catalogs uses of the aforementioned software for particle damper simulations.

PFC is said to be the most popular code for the field of geomechanics [67]. Some authors who study particle dampers also rely on the PFC3D[8] software [19,39,76].

Kozicki and Donzé [99] noted that coupling DEM with other simulation methods such as FEM is either not feasible because the software is commercial or time consuming for open source alternatives. They thus specifically developed Yade[9] to run coupled simulations of DEM and FEM inside a single framework. Yade is also used for particle damper DEM simulations [59,60]. Suhr and Six [94] use Yade to study different contact force models.

Another software which allows to model both DEM and FEM is Chrono [100]. The latter also has the ability to use the complementary method (CM) which uses Differential Variational Inequality (DVI) constraints to impede any particle interpenetration [97]. Fleischmann [97] compares granular direct shear tests results from the LIGGGTHS and the Chrono open source DEM toolboxes.

Klinge [58] uses LIGGGTHS[10] for their particle damper simulation. The approach of Sánchez et al. [10] is based on the Box2D[11] open source code which allows integration of the equations of motion. When using the DEM approach, it can be useful to rely

[8] http://itascacg.com.
[9] http://yade-dem.org.
[10] http://cfdem.com.
[11] http://box2d.org.

Table 1
Summary of the capabilities of selected DEM software.

	LAMMPS	LIGGGHTS	YADE	Chrono	EDEM	PFC
parallel	yes	yes	yes	yes	yes	yes
mpi/gpu	mpi & gpu	mpi	no	mpi & gpu	gpu	no
contact detection	grid, statistics-based	grid, Verlet, …	AABB	AABB, OBB	grid-based	cell-mapping, GJK
contact forces	linear, Hertz, molecular, interatomic potentials, …	linear, Hertz, cohesive, rolling, …	Hertz, Mindlin, linear, Coulomb capped	linear, Hertz, Coulomb	linear, Hertz, Mindlin, hysteretic, rolling friction, …	linear, Hertz, rolling, bond (BPM), …
open source	yes	yes	yes	yes	no	no
embedded FEM/CFD	CFD (LB)	CFD (SPH)	no	FEM	no	CFD/FD
can couple analyses	yes	yes	yes	yes	yes	yes
language	c++	c++	c++	c++	c++ API	c++ API
notes	targets molecular simulations	based on lammps		multibody dynamics engine with DEM-CM		

on a shape generator to create non-spherical particles. One such solution is the Automatic Sphere-clump Generator[12] (ASG). Certain software, such as Paraview, also facilitate the visualization of contact force distributions in a plane.

Each major particle software such as Yade, Chrono, PFC, LIGGGHTS, and EDEM exhibits a series of features and in most cases more than one is suitable for the application at hand. Table 1 attempts to provide a quick overview of their features, but the reader should bear in mind that it is by no means exhaustive. Although the table identifies software which is able to model molecular forces, this is not used for particle damper modeling [13]. A few abbreviations used in Table 1 are: the Gilbert-Johnson-Keerthi (GJK) collision detection algorithm for convex shapes; the Bonded-Particle Model (BPM) approximation of rocks as cemented agglomeration of smaller particles; the Finite difference (FD) method to solve discretized systems of equations; the MPI method for parallel computing on multiple machines; the Graphics Processing Unit (GPU) parallelization which uses the video cards of, usually, a single computer; the Application Programming Interface (API) which lets users program within and communicate with a dedicated portion of the software; Lattice Boltzmann (LB) methods which solve fluid dynamics problems using a cloud of particles; and, Smoothed-particle hydrodynamics (SPH) which solve fluid dynamics problems using a mesh-free particle-based approach.

Finally, the choice of software may be an important task, but carefully choosing and tuning the inner methods and parameters will provide most benefits.

4.7. General DEM identification

Ng [101] uses a DEM approach with a contact model made of a Hertzian normal force and a simplified Mindlin tangential contact. He studies the importance of different parameters on the results obtain for static drained and undrained shear tests. He thus observes the impact of changing four parameters, namely the shear modulus and density of the particles; a damping factor used with the mass to calculate the viscous damping coefficient; and, the timestep. He varies the parameters from 1/10 to 10 times their baseline values. He concludes that the influence of the input parameters is negligible within the range studied as long as a critical timestep is not surpassed. Finally, he finds that the parameter will have a considerable influence on the time required to reach a solution.

In his review of 238 papers, Coetzee [63] reports the identification procedures used by other researchers when characterizing DEM models. He mentions that there does not exist a standard procedure and thus there are many different methods used. They can be divided into two main categories: 1) the *direct measuring* approaches are the methods that individually identify the particle and contact parameters and then apply them in their simulations; and 2) the *bulk calibration* approaches are the methods that take results of the complete DEM simulation and from those calibrate all the parameters together. For the second method, Coetzee [63] warns that two different parameter sets may produce the same bulk response. This defeats the purpose of using parameters with a physical meaning, and may cause inaccuracy when the DEM method is used to model a case different from the one used during the parameter identification stage. The micro models, thus relying on direct measuring, have the limitation that the particle shapes and size, when not perfect spheres, are hard to measure and model. This thus renders difficult the micro modeling of their properties in these cases and bulk accuracy is not guaranteed. Using non-spherical particles can increase the computational cost by up to one order of magnitude.

Coetzee [63] also mentions that rolling friction is often used as an alternative to identifying the exact particle shape and size. He repeatedly mentions the importance of adjusting the parameters, such as the rolling friction, every time the shape of the particle is changed. Many identification studies he covers use the angle of repose of the granular material as the experimental data for calibration. The angle of repose is the maximum angle which can be formed between the horizontal plane and a pile

[12] http://cogency.co.za.

of granular material. A sample of other calibration methods are the hopper discharge flow; bulk compression; shear test; wall friction; cone penetration; bi- and triaxial tests; dynamic angle of repose and required power in a rotating drum; and, other in-house methods. An hourglass type of experiment can be useful to obtain two sets of data, which are the repose angle and the flow rate. He adds that smaller particles and particles with different shapes can lead to the same change in the effects when the modification of the number of contacts is changed equivalently. He also reports that for mixing experiments, the presence of sharp edges in the particles is an important factor to consider and has a much greater impact than the aspect ratio of the particle. The size of the particles is sometimes modified in order to reduce the computational time. However, this leads to the need to rely on the bulk calibration approach rather than on a direct measuring approach. In such a case, the operating conditions become important and the model may not remain valid outside of a restricted operating range. To that effect, Coetzee [63] mentions that scaling laws were developed by some authors. They allow to adapt the parameters of the size-changed particles to represent the ones with the original shape. These scaling laws require to also scale the structure geometry, and may thus not necessarily reduce the number of simulated particles. Scaling particles also has an influence on their interaction with air, power consumption, flow characteristics, and other aspects of the structure response. Scaling laws can be different for different authors and applications.

In general, the authors cited by Coetzee [63] warn to be careful when scaling as different aspects of the results can consequently change. Nevertheless, in order to reduce computational costs, a macro to micro scale one-way coupling is reported. In this simulation, the macro model contains only large spheres which then serve as input to a model with fine grain used in the locations of interest. Although not a parameter per se, the type of contact model and its behavior, such as whether the particles are allowed to exert tension forces between each other, should also be carefully thought through. As seen from the literature, there are many different contact force models. Some cases are reported where the linear contact model is as accurate as the Hertz-Mindlin.

When using the bulk identification procedure, Coetzee [63] recommends relying on more than one experiment and possibly isolating the parameters to identify. Doing so avoids calibrating the experiment instead of the material. The advantage of the bulk method is that it allows using larger particles than the real material. It also allows to identify parameters that may be nearly impossible to otherwise identify, such as rolling friction caused by material non-sphericity. Often, even when relying on the bulk method, some parameters are directly measured. Effectively, in the reported literature, most authors obtain their parameters from the literature and then proceed to a calibration process on a small selection of parameters. Commonly, an optimization algorithm is used and the experimental data against which the calibration is done depends on the study. Sensitivity studies are also often used to determine which parameters have a negligible influence on the object of investigation. These parameters of minor importance are then usually taken as constants, possibly from the literature. Coetzee [63] mentions that it is desirable to perform a validation test on the results obtained from the bulk method. Such a validation experiment should be as different as possible from the original calibration experiments to ensure that the model properly represents the material. He also reports that in some cases, changing one parameter, such as the sliding friction coefficient, can increase the sensitivity of the experiment to another parameter. For example, the values of the coefficients of restitution and rolling friction may have no influence on the granular material behavior until another parameter changes. The fact that certain parameters may not affect at all the outcome of a specific test indicate that great care must be taken to assess the sensitivity of the tests used to identify the model. Another example of effects that can cancel each other out is the contact stiffness which by decreasing can increase the number of simultaneous contact of each single particle. Some authors will proceed step-by-step with different experimental data to progressively calibrate all the parameters. Coetzee [63] also highlight that the influence of the inter-particle friction coefficient can become negligible in cases where a bond contact model is used. Such model uses a stiffness force up to the point where Coulomb static friction becomes larger. Finally, he proposes a 6-step parameter identification approach for DEM which goes as follows:

1. model the particle shape and size, eventually using clumps;
2. determine the particle-wall friction coefficient through an inclined plane test;
3. use the DEM-obtained packing fraction to tune the particle density according to the experimentally measured bulk density;
4. perform a bulk uniaxial constrained compression test to iterate to a valid particle stiffness value;
5. perform a direct shear test to obtain the bulk friction coefficient and iterate for the proper particle friction coefficient.
6. recalibrate the density with the new friction coefficient

This method allows to obtain every parameter of a DEM simulation except the particle-wall stiffness and the coefficient of restitution. For his purposes, he sets the latter to the critical value of 0.8, based on visual inspection. His model neglects rolling friction and he takes the particle-wall stiffness as being 10 times particle-particle stiffness.

As for direct measurements, Coetzee [63] reports different methods used in the literature. The use of a special apparatus allows measuring the particle-particle sliding friction with displacements and normal loads varying between 1 μm and 500 μm and different normal forces. Other approaches glue the particles to a plane which is then slid against another plate of the same material as the particles. Particle density is also measured with a pycnometer. High-speed cameras are used to determine the coefficient of restitution between the particle and the wall. A double pendulum with a high-speed camera allows to obtain the coefficient of restitution between particles. Other cases use a drop test on the particles and record both rotation and velocity changes to obtain the coefficient of restitution between the particle and a wall. The details of the latter method are given by Hastie [102]. Coetzee [63] reports that it was also shown that the coefficient of restitution changes with particle shape, impact

velocity, and impact angle. It is not uncommon that the value obtained by direct measurement has to be modified to allow the DEM model to properly reproduce the bulk calibration tests. In an uncommon test, the rolling friction coefficient of a granular material is measured from the inclination angle at which a steel ball begins to roll on the granular bed.

Finally, Coetzee [63] reports that variability of the properties between one particle and the others can also have a considerable influence on the modeled results and should be assessed. However, this is not commonly covered in the literature. He reminds that particle shape(s) and size(s) should be the first parameters to be identified. He also mentions that the most popular approach is to bulk calibrate and the most popular test to do so is a combination of hopper discharge and repose angle, mentioned here earlier as the sandglass experiment. However, he warns that further validation is necessary to ensure the proper material values were thus obtained.

4.8. Particle damper DEM identification

Lu et al. [6] uses DEM to model a particle damper and validates it experimentally. Although not explicitly mentioned, it appears from their article that little or no calibration was conducted on the model parameters and that standard literature values were used. A prior article from the same group concerning the same experiments [103] does not clarify the origin of these parameters. It, however, gives a criterion for the minimum acceptable timestep. Yet another article on a very similar experiment [104] indicates that they obtain their coefficient of restitution of steel against rubber from the work of Li and Darby [105] which in turn refers to an article from 2005 that was apparently not published. All this leads to believe that the group of Lu is using direct measurements or literature data for their parameters. That supposition is supported by the article of Lu et al. [106] which mentions that the parameters for steel come from the work of Masri and Ibrahim [1].

Els [76] starts with Young's modulus and Poisson's ratio taken from the literature. He also uses other parameters based on the literature. He then iterates over different friction and damping coefficients until the DEM results match those of his prior experiments. He confirms the validity of the obtained coefficients because they correspond with the prior work of Wong et al. [19]. Finally, Els [76] states that damping has a minor impact of the efficiency while friction is the dominant factor.

In their work, Wong et al. [19] measures the coefficients of friction and restitution for the particles of a particle damper. They identify the friction by sliding different types of steel spheres against a steel plate. They note dependence on velocity and indicate that a damped shear stress model may be adequate if these effects are important for the particle dampers. They also note a dependence of up to 20% on grain orientation of the steel plate. They also note a strong influence of the type of steel sphere, which differ, for example, by coating. They rely on particle-plate values for both particle-plate and particle-particle values of the DEM simulation. They justify this choice by stating that 1) the scatter is already so large that it probably overlaps possible differences, and 2) the contact between two spheres would be a point contact, which is almost identical in shape than the contact between a sphere and a plate. For the coefficients of restitution, they use nylon fishing line to create pendulums. These pendulums allow to produce the impact between two spheres. They record the rebound of the spheres with a 900 fps camera and from that obtain the particle-particle coefficient of restitution, with reserves on its accuracy. For the particle-wall coefficient of restitution, they perform a drop test where the spherical particle is allowed to drop on a horizontal steel plate. The impact interval between two contacts is measured with a piezoelectric transducer and from this data the coefficient is obtained. As for stiffness values, they obtain them from available literature data. They compare their DEM simulation using the obtained parameter values to experimental data. The measured power correlates reasonably well. They conclude that: the linear contact model gives results similar to those obtained with the Hertz-Mindlin method; contact stiffness can strongly influence power dissipated; although friction is the dominant dissipation contributor, the value of its coefficient has little influence on the dissipation itself; energy dissipation is harder to model at the onset of the simulation when the behavior is still transient; and finally that there is still a lot to discover about particle damping. The coefficient of friction having little influence even when friction is the dominant dissipation contributor may sound counterintuitive, but this is explained by the large quantity of tangential impacts which tend to dissipate the same quantity of energy whether each attrition case is individually stronger or not.

Similarly, Masmoudi et al. [60] also find negligible impact of the coefficient of restitution on the energy dissipated by their particle damper. They use Young's modulus and Poisson's ratio from the literature. They also give seemingly standard coefficients of restitution, but then use a value of 10^{-6}, chosen arbitrarily to ensure inelastic collisions. They corroborate the DEM results to their experimental data prior to performing a parametric study. Their parametric study covers the total particle mass, the number of particles, the density, the radius, the coefficient of restitution, and Young's modulus. The outcome is that, apart from the total mass, the parameters can vary within a wide range of values without influencing the amount of dissipated energy. The total mass is, instead, linearly correlated to the dissipated energy.

Xia et al. [5] test a particle damper made of 2 mm spheres with the DEM approach. They list all the parameters used by the method, but it is not clear whether they were calibrated or taken from the literature.

Xiao et al. [39] have a contact model which is based on the shear and elastic moduli of the material and its Poisson's ratio. Their coefficients of friction and of restitution and other parameters are given and are plausibly taken from the literature. It appears that they do not further calibrate these parameters.

The contact model in the DEM implementation of Wang et al. [56] uses the coefficients of restitution and friction which they say can be found in technical manuals. It appears that they do not further calibrate the parameters to match their experimental data. They take the coefficient of restitution from the work of Stevens and Hrenya [107]. The latter conduct an experimental study which allows them to obtain both the coefficient of restitution and the collision time of impacting spheres. They then use

Fig. 5. Impact damper design of Olędzki et al. [11]. Reprinted with permission from Elsevier.

Fig. 6. Damped glider tube of Olędzki et al. [11] (see arrow). Reprinted with permission from Elsevier.

the data to evaluate the capability of different contact models to reproduce the collision behavior and find satisfactory results with the Hertz contact model.

Sometimes the granular material particle diameters are only defined by their mesh size, as done by Wang et al. [9].

Duan and Chen [57] rely on the material parameters to set up their DEM. As mentioned before, they also use a velocity-dependent coefficient of restitution. Nonetheless, they tune their DEM simulation by introducing an empirical coefficient which corrects both normal and tangential damping coefficients of the contact model for both particle-particle and particle-wall contacts. As such, they minimize the error of their own indicator of power dissipation, the loss power, measured from the experimental and DEM results.

5. Testing of particle damper configurations

Olędzki et al. [11] insert an impact damper inside the tube of a motorized glider and achieve a reduction of roughly three times of the vibration amplitude of the tube. The impact damper design and its position inside the tube are shown in Figs. 5 and 6. Olędzki [108] runs tests with a vibration generator at null, 3 Hz, and 10 Hz bandwidths to identify the magnitude of the registered vibrations.

To test the damping provided by an impact damper, Akl and Butt [109] and Butt and Akl [110] excite a brass tube in the horizontal direction to minimize the effect of gravity. They constrain the beam at both ends. One end is only allowed to rotate about the vertical axis and the other end is only allowed to move elastically in the horizontal direction. Their experimental setup uses steel billets having masses of 907 kg to ensure that the vibrations are isolated. They test their apparatus, with the damper, by recording the vibration response of the beam and the billet under a random excitation going up to 625 Hz. To do so, they use multiple accelerometers to obtain the frequency response in both vertical and horizontal directions. They thus identify that the system's behavior is linear up to 200 Hz. Force transducers were also installed at the point of excitation, which is the shaker, and at the position of the impact damper. They then conduct sine sweep tests to identify the response with the damper activated in two positions, with different masses, and clearances. They also test with the damper particle immobilized to obtain a baseline for comparison. They keep the sweep rate below a minimum recommended from the literature to ensure minimal distortion.

Akl and Butt [109] thus analyzed the response of the beam to its first three natural frequencies with a sinusoidal excitation sweep. They also report prior results from the literature which agree with the intuitive idea that the damper should be placed away from the nodes of the mode shapes to achieve optimal damping. Butt and Akl [110] obtained considerable damping for

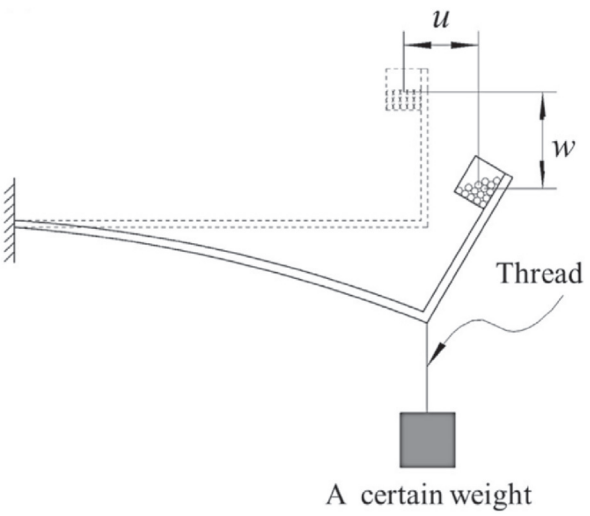

Fig. 7. Horizontally and vertically vibrating beam of Wang et al. [56]. Reprinted with permission from Elsevier.

their 1.37 kg tube using lightweight single particles ranging between 7.6 g and 17.1 g. These correspond to mass ratios μ going from 0.006 to 0.012. They report damping the undamped resonance acceleration response of 177 m/s^2 down to 29.4 m/s^2 using a mass ratio of only 1%. The weight of the particle casing is apparently not considered in the analysis and they report that both particle mass and its leeway inside the damper influence the efficiency.

Ehrgott et al. [52] used a test fixture to measure the damping of different modes of the turbine seal of a space shuttle. They find damping ratios that vary between 0.32% and 2.38% depending on the excitation frequency. Their undamped structure is reported to have a 0.1% damping ratio, although it is not clear at which frequencies this value is valid. The masses of the different parts involved are not given.

Wang et al. [56] perform numerical and experimental tests of a particle damper subjected to vibrations in both horizontal and vertical directions. The beam which provides these dual vibrations is shown in Fig. 7. They measure the beam response using a scanning laser vibrometer. The vibrations are induced by initially hanging a weight from the beam and then abruptly releasing it. They repeat each test six times at different initial amplitudes. They find that the specific damping capacity (SDC) Ψ is highly nonlinear and thus the velocity decay in time cannot be represented by a straight line on the time-velocity plot. They define the SDC as

$$\Psi = \frac{\Delta T}{T_{\max}} \tag{5}$$

where $T_{\max}$ is the maximum kinetic energy attained during a cycle and ΔT is the dissipated quantity during the same cycle. For optimal conditions, when the particles move together, the equation can be rewritten as [17,56],

$$\Psi = \frac{\dot{x}_i^2 - \dot{x}_{i+1}^2}{\dot{x}_i^2} \tag{6}$$

where $\dot{x}_i^2$ is the maximum particle velocity at cycle i. They also find a threshold where, to produce efficient damping, the particle moving vertically must have an acceleration large enough to overcome gravity and reach the ceiling of their cavity.

Wang et al. [56] mention that prior research studied the SDC of the particle damper as a function of four variables: 1) mass ratio; 2) dimensionless impact clearance; 3) dimensionless structure acceleration amplitude; and 4) effective coefficient of restitution. They use a DEM approach to perform a parametric study of the SDC as a function of more parameters. As noted by other authors, they also find a negligible sensitivity between the coefficient of restitution and the SDC. Upon further investigation, they realize that this is due to a compensation of the change in the coefficient of restitution. As the coefficient increases, less energy is lost in a single collision. However, this also causes a higher velocity which then causes more dissipation by friction and more contacts. They also mention that particle-particle interaction is the main source of energy dissipation while particle-wall interactions rather serve to transmit energy between the structure and the damper. Interestingly, they find that increasing the friction coefficient reduces the damping capacity. Their observations bring them to deduce that with a higher friction coefficient, the particle velocities are reduced. As a consequence, the number of particle inelastic collisions is also reduced.

Wang et al. [56] also find that, as the horizontal to vertical excitation ratio is increased, so does the damping capacity. Investigating, it is found that the increase comes from friction dissipation and they explain that this is due to the presence of oblique collisions and rolling friction caused by the combined directions of excitation. They also investigate the influence of the mass ratio, and the horizontal and vertical cavity clearances. Finally, they suggest that particle dampers should be designed by also taking into account the magnitude of the expected accelerations the structure will be subjected to.

Fig. 8. Damper proposed by Du and Wang [46]. Reprinted with permission from Elsevier.

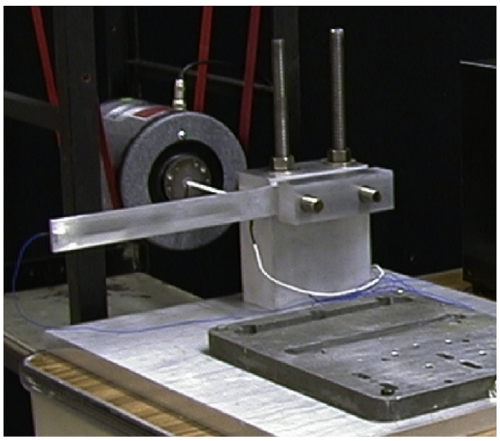

Fig. 9. Test fixture of Bryce L. Fowler [18]. Reprinted according to the terms of the Defense Technical Information Center. U.S. Government Work.

Du and Wang [46] propose a new concept of particle damper which is a combination of the impact damper and the particle damper. They name it the fine particle impact damper and they test it both numerically and experimentally on a cantilever beam. The damper is shown in Fig. 8. Their FPID damper is significantly more efficient than the equivalent single particle impact damper. They attribute this to the plastic deformation of the soft particles which make up the FPID.

The experimental configuration of Bryce L. Fowler [18] for testing a single beam under load is shown in Fig. 9. It consists of a shaker-excited cantilever beam with particle damper and accelerometer placed near its tip to retrieve the first mode of vibration. The results from Bryce L. Fowler [18] indicate that the undamped beam and the beam with an added mass equal to the particle's mass have similar response amplitudes. The added mass lowers the resonance frequency by roughly 5%. Their use of a single sphere as a damper barely reduces the response amplitude at resonance while the use of 64 spheres having an equivalent total weight reduces the response amplitude at resonance to less than half the undamped response. Information about the mass of the undamped beam is not given, thus comparative efficiency cannot be obtained.

The experimental configuration of Saeki [43] which allows them to test a particle damper having multiple units and applied to a horizontally vibrating system is shown in Fig. 10. It represents the multi-unit model shown in Fig. 11. Their cavities are made of acrylic resin.

For excited particle beds, Wildman et al. [111] created two-dimensional particle beds using glass walls barely thicker than a single particle. They excited these beds with a shaker and obtained motion information using a high-speed camera and a frame-by-frame particle tracking software. They focus their measure on the particle packing density and the temperature profiles, where they refer to the kinetic energy of the particle bed as its granular temperature. In three dimensions, cameras are no longer able to capture the motion of the particles. Another technique is thus used by Wildman et al. [111] for 3D. It consists of tracking a single positron-emitting particle from the bed. They let the experiment run long enough to allow it to cover the whole cavity and then recreate the packing fraction and granular temperatures.

Marhadi and Kinra [112] rather measure the decay of a freely vibrating beam to which an initial displacement has been applied using a magnetic coil. It is not clear whether the magnetization of the particles also has an influence on their results. Their experimental setup is largely inspired by the work of Friend and Kinra [113].

Xu et al. [7] find additional beam-damping from their longitudinal cavity configuration of a non-obstructive particle damper. They mention that the additional damping comes from the longitudinal strain of the beam which induces shear motion in the granular bed. The traditional and longitudinal NOPD configurations are shown in Figs. 12 and 13, respectively. Their experi-

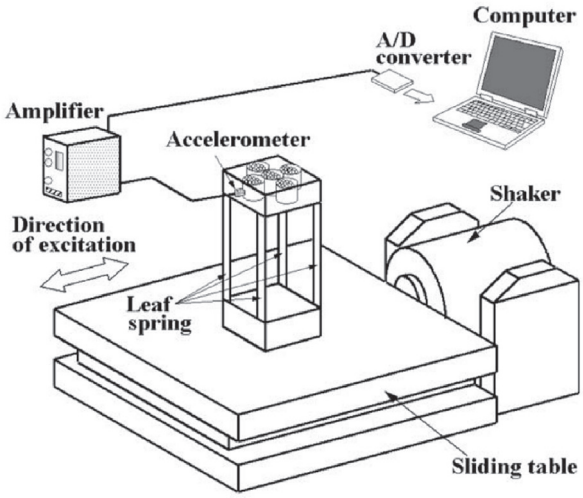

Fig. 10. Test setup of Saeki [43]. Reprinted with permission from Elsevier.

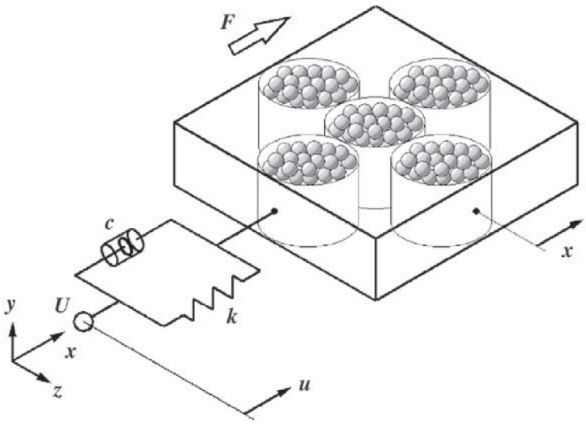

Fig. 11. Model of Saeki [43]. Reprinted with permission from Elsevier.

mental setup is shown in Fig. 14. From their experiments on the longitudinal configuration, they conclude that their numerical model is able to predict the damping of the bending modes they examined. Their model, as expected, does not reproduce the torsional mode. The damping at each mode is considerable and becomes stronger for higher frequencies. Torsional damping is, however, almost absent. They also conclude that shear friction in their longitudinal configuration is the dominant energy dissipation factor, as opposed to the traditional transverse configuration where impact is the dominant dissipation cause.

Xiao et al. [39] experimentally test a particle damper configuration used to damp vibration in a gear. A photo of the system is shown in Fig. 15. They conduct their tests 5 times to obtain the average response and reduce statistical errors. The masses of the compartments they use to hold the beads in the cavities vary from 0 g to 62.7 g. They find an optimal packing ratio between 60% and 80%, depending on the gear angular velocity. They model their gear as a 2 DoF planar system with viscoelastic joints acting in the axial and in the radial directions of the gear. They test different gear loading moments.

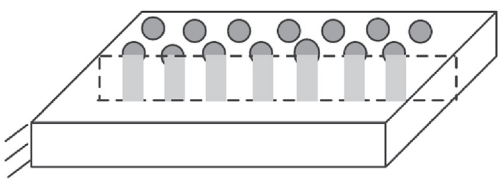

Fig. 12. More common transverse beam particle damper shown by Xu et al. [7]. Reprinted with permission from Elsevier.

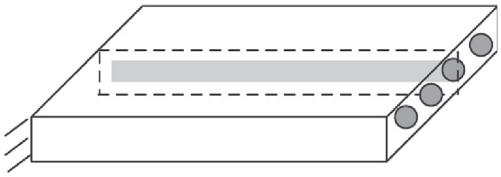

Fig. 13. Innovative longitudinal beam particle damper configuration of Xu et al. [7]. Reprinted with permission from Elsevier.

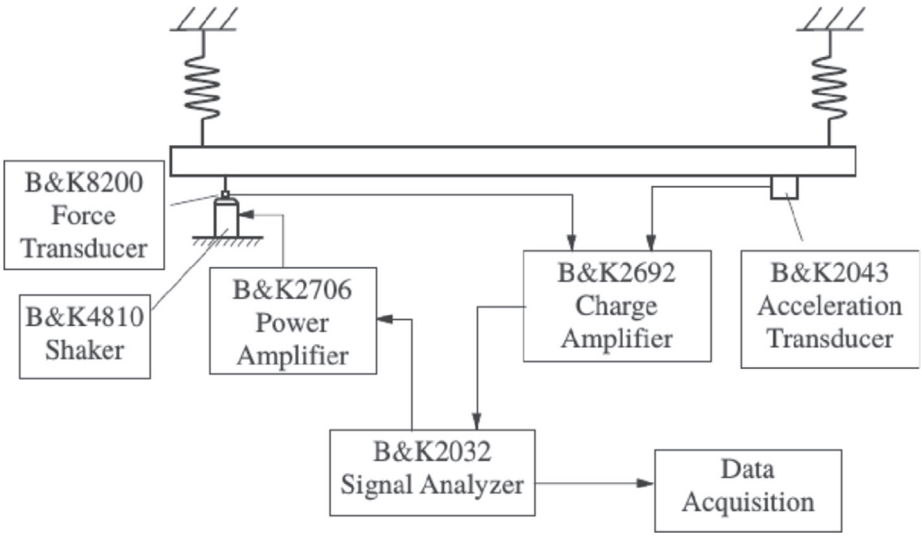

Fig. 14. Experimental configuration of Xu et al. [7]. Reprinted with permission from Elsevier.

Duvigneau et al. [114] attempt to damp the oil pan of an automotive engine by embedding a particle damper inside of it. Their motivation is to reduce noise emissions from the pan. They measure the oil pan's response to shaker-induced excitations with a scanning laser vibrometer. The shaker is actually attached in series with an impact hammer and used solely to impose controlled and repeatable excitation without affecting the boundary conditions. During those tests, the pan is hung with synthetic strings to ensure a perfectly horizontal position and free-free boundary conditions. They also show that augmenting the quantity of the granular matter does not drastically improve damping performance. They also find a significantly more important damping when using sand than when using the same amount of water. They contemplate the use of honeycomb in order to create a lighter oil pan while also allowing particle damping effects. An idea of their test setup can be grasped from Fig. 16.

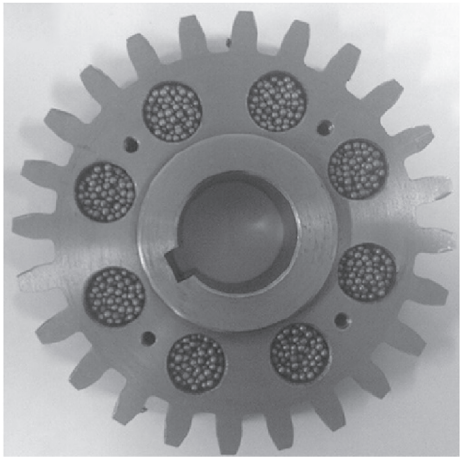

Fig. 15. Experimental configuration of Xiao et al. [39]. Reprinted with permission from Elsevier.

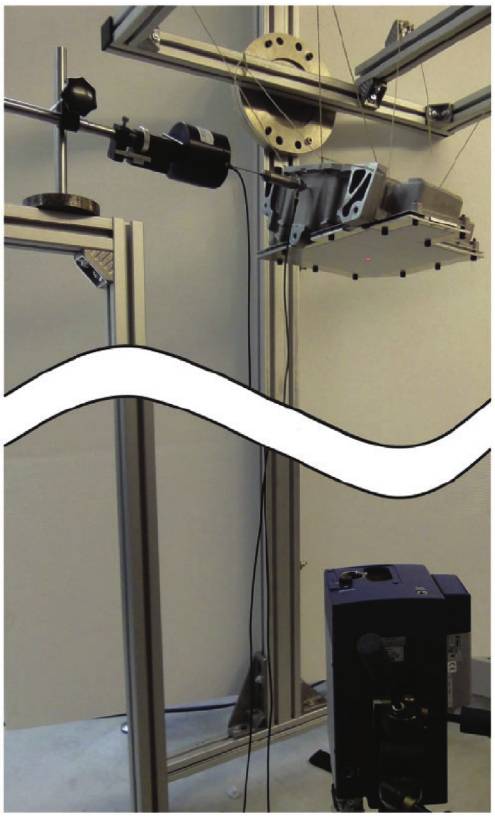

Fig. 16. Experimental configuration of Duvigneau et al. [114]. Reprinted according to the terms of the STM quantity limits for gratis permission.

Els [80] performs tests on the influence of centrifugal loads on particle dampers. His experimental configuration models a damper that would be attached to the tip of a helicopter blade and act vertically. Having a rotating test beam, the author isolated it from aerodynamic effects by enclosing it in a larger cylinder. He focuses his analysis only on the bending mode of the beam. The cavity is cylindrical. He conducts a mathematical analysis of the beam with and without the particle damper's cavity to assess the influence of the rotation velocity and cavity mass on the natural frequency, stiffness, and damping of the beam. This allows him to justify the use of an equivalent single DoF model.

In order to assess the influence of the particle damper in isolation from changes in mass, Els [80] uses 4 different cavities with nearly identical masses and changes the number of particles while keeping a constant total particle mass. He evaluates the damped responses in terms of peak acceleration, damping coefficient, and change in effective mass. To measure the height of the filled portion of the cavity, he relies on repeated DEM simulations where the particles are allowed to settle under gravity and from which he takes the average height. He finds that the aspect ratio, the magnitude of the centrifugal load, and the number of particle layers have non-negligible influence on the performance of the damper. The centrifugal load also influences the ability to damp vibrations of smaller amplitudes.

In a follow-up, Els [76] chooses to use a single DoF equivalent model of his rotating beam in a DEM simulation. His DEM implementation uses the Hertz-Mindlin contact stiffness and viscoelastic damping. He finds very good correlation between experimental and numerical results at different beam rotation velocities.

Lei and Wu [115] recall that the particle damper should be placed at the position of maximum vibration velocity. They also find from their experiments that different magnitudes of contributions to damping come from the particle-particle collisions, friction, and interaction with air. The importance of these contributions are given against vibration velocities in Table 2. Their damper consists of four cylindrical holes made in the original beam. They each have a 10 mm diameter and a 13 mm depth. Their numerical approach couples a beam finite element software with a numerical routine which adds the analytically calculated additional equivalent viscous damping coefficients. They rely on tungsten powder or steel spheres as the damping material, depending on the test. They conduct their experiment by exciting the beam with a harmonic force produced by a shaker. They obtain the force and acceleration signals through a force sensor and an acceleration transducer, respectively. This is shown in Figs. 17 and 18.

Lu et al. [106] build a 1:200 scale model of a 76-story building by following the similitude guidelines from the American Society of Civil Engineers (ASCE). They then use the model within an aeroelastic study of the building response inside a wind tunnel. Their configuration consists of a suspended container box attached by four strings to the top of the building model.

Table 2
Influence of vibration velocity on damping contributions according to Lei and Wu [115].

velocities (m/s)	1st contrib.	2nd contrib.	3rd contrib.
below 0.03	air	collisions	friction
[0.03, 0.16]	collisions	air	friction
beyond 0.16	collisions	friction	air

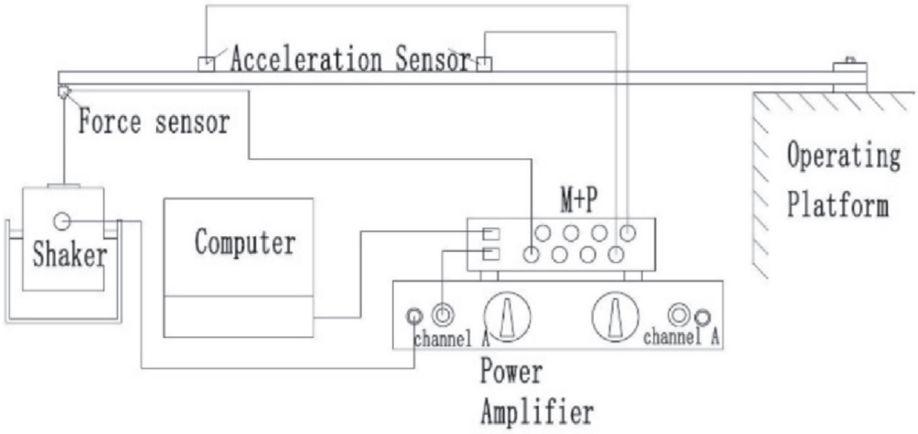

Fig. 17. Experimental schema of Lei and Wu [115]. Reprinted with permission from Springer Nature.

The box hosts spherical particles which provide damping and the natural frequency of the whole damper can be tuned by changing the length of the strings. The configuration of their experiment can be seen in Fig. 19. They show that the acceleration and displacement responses of the building are diminished by the presence of the tuned particle damper by a value which significantly depends on the string length.

In prior work, Zheng et al. [103] tested the efficiency of a particle impact damper on a three story scaled building. The damper is made up of 4 steel containers each having 63 steel spheres of 50.8 mm diameters and is placed on the roof of the building. The total mass of the damper is 135 kg, excluding the cavity, and the building weighs 6 metric tons. The building was also designed to have its first three natural frequencies between 1 Hz and 5 Hz.

Yet in another similar work by the same group, Lu et al. [104] test the impact of buffering the particle damper by adding a 20 mm rubber padding to the cavity of their top-floor building damper. They find improved damping when using the buffered version of their damper. They also indicate that the frequency for which the damper is placed at the position of maximum displacement is better damped than the other frequencies.

Salvino et al. [116] experimentally test two different particle materials to damp a box beam. They find little difference between the damping performance obtained from shredded navy tiles and polyethylene beads. They evaluate the damping of the beam using the wave method of McDaniel et al. [117] which allows evaluation of the loss factor over a continuous range of

Fig. 18. Experimental configuration of Lei and Wu [115]. Reprinted with permission from Springer Nature.

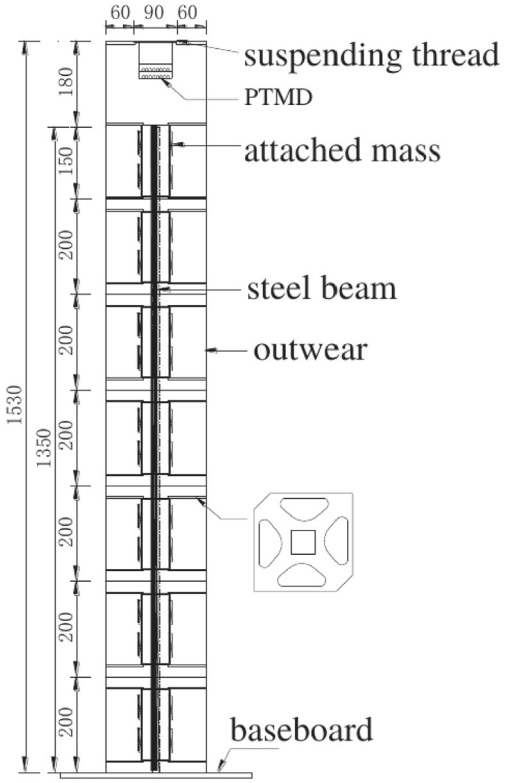

Fig. 19. Experimental schema of Lu et al. [106].

frequencies. This latter method also allows to generate of a wave number versus frequency acceleration map to simultaneously identify the nodes, frequencies, and amplitudes of the response.

Michon et al. [8] perform a study where they use hollow particles instead of typical hard particles used in particle dampers. They rely on such hollow particles to limit the weight impact of the damper, intended for space applications. They conduct a three-step experimental campaign: 1) They identify the behavior of the damper alone, with and without honeycomb fillings, and excited by a shaker undergoing a sine sweep of frequencies. This leads them to realize that the individual cells of the honeycomb structure can be modeled as spring-mass-damper systems. 2) They change the honeycomb structure for a more realistic structural part made of aluminum. Being careful to remove inertial effects, they are then able to plot displacement-force hysteresis curves of the damper at different excitation frequencies. They also insert a piezoelectric load cell between the shaker and the structure to obtain the transmitted force. The obtained force curves are all ellipsoidal. This implies that viscous behavior is dominant in their novel particle damper. In addition, no resonance is identified up to 3000 Hz, which brings the authors to conclude that the damper has no stiffness. They find that effective particle mass and damping coefficient are functions of frequency and filling ratio. And, they identify the damping coefficient from the area of dissipated energy in their hysteresis loops. 3) They evaluate the response of a honeycomb cantilever beam with cells that contain the particles. This experimental configuration is shown in Fig. 20. They excite the free end of the beam with a shaker and rely on four accelerometers to obtain the acceleration response of the beam. They then use a harmonic finite element beam model with the equivalent mass-spring-damper systems previously identified to study the response of the cantilever beam to a series of excitation frequencies and obtain a good correlation in the predicted damping ratios. The concept of their model is shown in Fig. 21.

Michon et al. [8] find that the optimal filling ratio, defined as the space occupied by the particles envelope, varies between 67% and 90%. The lower values apply to higher excitation frequencies, and vice-versa. They also find that the first vibration mode of their particle-filled honeycomb cantilever beam remains undamped even with the presence of the hollow particles.

Simonian [14] studied the response of a spacecraft antenna protruding from a cantilever beam. He uses twang tests to assess the efficiency of his particle damping solution. He describes this method as applying a load at the end of the antenna and suddenly releasing it to observe the free vibration response.

While conducting their analysis of a vacuum particle damper, Szmidt and Zalewski [44] rely on 3 laser displacement sensors to measure the vibration response. They use an electric motor to rotate an unbalance mass and thus generate parasitic vibrations at the end of a cantilever beam. Their beam consists of a small steel core inserted into a particle-filled envelope under vacuum. That envelope is the damper. They repeat each experiment 3 times to ensure good repeatability. Their experiment consists of an

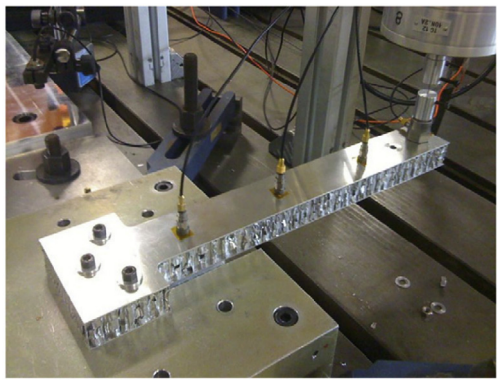

Fig. 20. Experimental setup of Michon et al. [8]. Reprinted with permission from Elsevier.

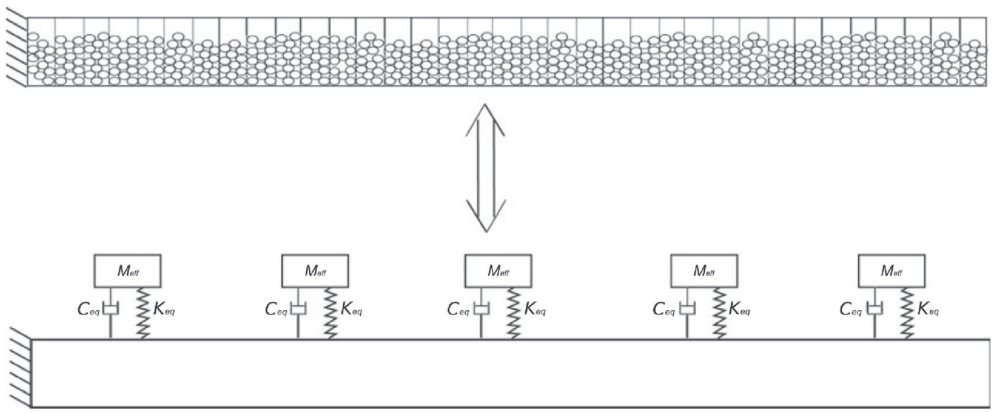

Fig. 21. Numerical schema of Michon et al. [8]. Reprinted with permission from Elsevier.

extension of the work of Zalewski and Szmidt [118] which presents the characteristics of the beam particle damper with more detail.

The use of a vacuum within particle dampers allows to reverse the state of matter transition from fluid-like back to solid-like state [31]. Such a process is referred to as a jamming transition [22,27]. The motivation for this process is that the literature demonstrates that the most effective damping usually occurs when the granular material is in the solid-like state. More precisely, the material should be near the transition to another state where inter-particular rolling begins to occur [29]. Some studies define these transition states as suspended states, namely the Leidenfrost effect and the biconvective state. These suspended states are found to be most effective at damping [23,26]. They also maintain a solid-like behavior for the majority of the granules. Nevertheless, the definition of the different states is subject to different interpretations. As such, definitions based on the relation between the magnitude of the excitation acceleration and the length of the cavity were proposed by Salueña et al. [2]. They use the name convective state for the fluid-like state which occurs after transition from the solid-like state is complete.

For impact damping, Olędzki et al. [11] conclude from their simulations that the value of the coefficient of restitution of the material has negligible influence on the efficiency. They find that an influential parameter on the resonance amplitude of their metal tube is the clearance in which the impact damper is allowed to travel. The tube they damp is 2 m long and has a reduced mass of 0.8 kg. The damper has a mass of 0.4 kg. The original mass of the beam is not reported in the paper. The undamped bending resonance amplitudes was roughly 10 mm while the damped amplitude can be as low as 1 mm, depending on the damper gap.

On a contrary note, Olędzki [108] reports prior art which states that the coefficient of restitution is the main influencer of the single particle impact damper. He still uses a single particle impact damper. He argues that because the coefficient of restitution has a strong influence and that it cannot realistically be made lower than 0.3, a possible solution to obtain good damping at low mass ratio μ is to rely on Coulomb friction. He tests his design, which has a 17 Hz first natural frequency. Olędzki [108] finds that the impact damper is most effective for restrained excitation bandwidths. The equivalent mass of the damped beam where the damper is attached is 700 g while the mass of the impactor, a steel ball, is 64 g. The container mass is roughly 32 g.

For multiple impactor damping, Iwata et al. [119] attempt to optimize the mass distribution of a multi-unit single-particle damper. The excited plate they damp weighs 2.26 kg and with a total combined mass ratio of 0.12 three vibrators can consider-

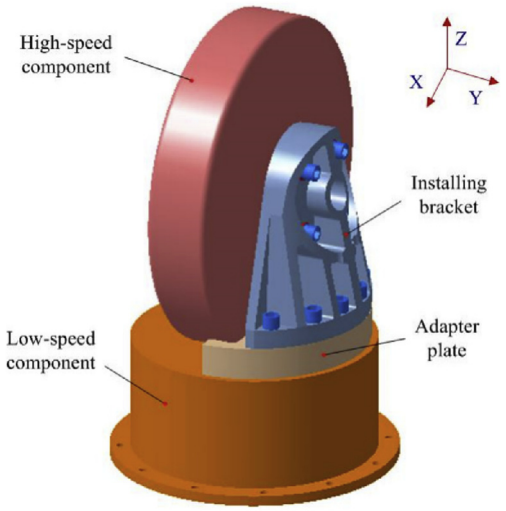

Fig. 22. Main structure of Wang et al. [9]. Reprinted according to the terms of the Creative Commons License.

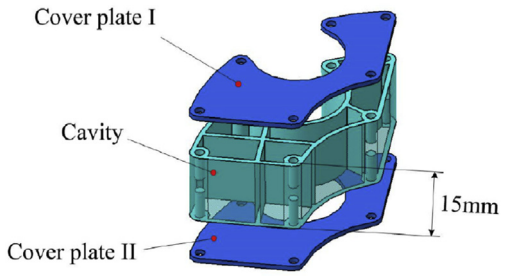

Fig. 23. Damper geometry of Wang et al. [9]. Reprinted according to the terms of the Creative Commons License.

ably reduce the vibration amplitude. From his experimental and DEM simulation campaign, Saeki [53] finds good attenuation of a horizontal system's response for a particle damper with mass ratios of 0.092 and 0.138. He also tests different materials such as lead, steel, and acrylic resin to find out that they have a notable but limited influence on the results. In the paper, it is not clear whether the mass of the particle container, the cavity, is considered as part of the main structure or of the damper. The length of the cavity is, however, found to be an influential parameter. For his multi-unit particle damper, Saeki [43] also reports from his experimental tests that the presence of the particle damper reduces both the resonance frequency and amplitude. He notes a clear influence of the mass ratio and the number and radii of the cavities on the response amplitude. The higher mass ratio does not always provide the better damping. The same also applies to the number of cavities. For example, a smaller number of cavities can provide a better damping at high response amplitudes. The mass ratios he tested are 0.058 and 0.098. Overall, there is a complex relationship between the parameters and the numbers of particles that become in contact with the walls of the cavities and thus on the damping properties.

In both 2D and 3D experiments of a granular bed, Wildman et al. [111] find that packing fraction increases with height within the cavity until it reaches a plateau and drops. They also report that in some states of the particular bed some properties granular gases of these particle beds are similar to those of fluids. However, in most states, they differ. For example, the velocities at small wave numbers differ from the fluid's velocities, as they are anisotropic.

Trigui et al. [17] study the effect of a particle damper located on the tip of a cantilever beam. They first identify the beam's response and natural frequencies with an equivalent dead mass positioned at the location of the damper.

Wang et al. [9] test their structure on a shaker. They use the shaker to generate a sine sweep over the frequencies of interest and collect the responses of the structure at locations of input and output using accelerometers. The structure is to be used on a spacecraft and is shown in Fig. 22. They test each condition 3 times and take the mean response as the final value of interest. Their damper geometry is shown in Fig. 23 and its location on the structure in Fig. 24.

As complementary summary, Tables 3–5 provide an overview of the particle dampers tested in the literature. They give a chosen sample from the articles cited, as in some cases, more conditions or devices are tested within a single article.

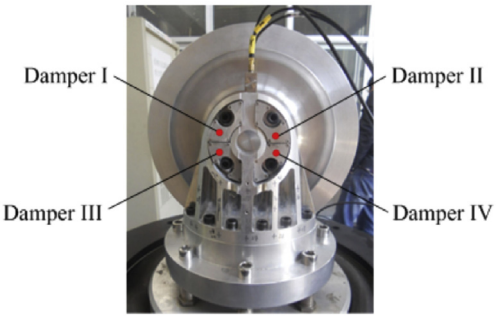

Fig. 24. Damper installation of Wang et al. [9]. Reprinted according to the terms of the Creative Commons License.

5.1. Influence of direction and disturbance vibrations

Although usually ignored and sometimes dismissed as negligible, vibrations in a direction different than that for which the damper is designed may have an impact. This subsection provides an overview on the matter.

Wang et al. [9] study the vibration response of a spacecraft component in 3 directions using accelerometer readings for each direction. The response without the particle damper has a peak in two of the three directions for the fundamental frequency. Their findings are that their particle damper is effective at simultaneously damping the response in both directions over a range of frequencies.

Wang et al. [56] notes that the main effect of bidimensional excitation is the diagonalization of the resulting particle motion. Thus, their damper remains effective when subjected to perpendicular excitation of increasing magnitude. These excitations have the same phase and period in both directions. The impact of gravity increases dissipation when vibrating in the horizontal direction because oblique impacts between the particles are favored. Effectively, such oblique impacts are much less frequent under pure vertical excitation.

Lu et al. [13] model a particle damper excited in two directions and characterize its behavior while varying diverse parameters using DEM. It takes them 1000 natural periods to reach a stable response. When the lateral vibrations in both directions are correlated, their effect is to diagonalize the response trajectory. This corresponds to the response that would occur if the container was rotated. This reasoning only applies if the vibrations are correlated because, otherwise, the trajectory of the particles is rather circular. They measure damping efficiency with the decay of the cross-correlation velocity between the particles. As such, they find better damping for excitation in two directions when using cylindrical containers. They estimate that this is due to the symmetric shape which favors more collisions.

Suyama et al. [15] perform tests on a turning machine. They damp the tool holder and monitor vibrations in the radial and tangential directions. They, however, only report the radial vibration response and do not mention implications of the bidimensionality of the excitation. Darabi [77] performs DEM simulations for viscoelastic particles making up a particle damper. He finds that the amount of energy dissipated by friction is almost equal between horizontal and vertical excitation of the damper cavity. However, the overall energy dissipation by the damper is up to 3 times more when excited in the vertical direction. The influence of his excitation direction is enough to change the particle bed behavior from fluid-like to gas-like. Oyadiji [123] conducts separate testing for horizontal and vertical excitation of a particle damper. The particles are inserted into a hollow rectangular beam. The frequency response of his free-free beam between 0 kHz and 2 kHz is considerably and congruently damped for excitation in both directions. Nevertheless, the size of his particles and orientation of his excitation has an influence on the relation between loss factor and frequency.

Also, Lu et al. [96] provide results for a particle damper excited simultaneously in two directions which are not that of gravity under random stationary excitation. Their DEM-based parametric study indicates that the optimal container size in each direction must be neither too small nor too large. The former would impede inter-particle motion and the latter would cause too long travel time between the walls of the container.

Els [80] also considers the effect of bidimensionality excitation with his particle damped rotating beam. The rotating axis and the first bending mode vibrations are vertical. The centrifugal loads are constant but also induce higher modes of vibration for both bending and torsion of the beam. These higher modes are of smaller amplitudes and have frequencies approximately one order of magnitude higher. He then investigates the effects of the centrifugal forces, which are correlated to the geometry of the containers. Little attention is given to the higher vibration modes.

Panossian [124] tests multiple modes of a space shuttle engine vane for the vibration attenuation in both bending and torsion. His tests are conducted on a free-free support and excited by a shaker. Little attention is given to responses from excitation or vibration in two simultaneous directions but damping is significant at all modes tested. Similarly, Chen and Georgakis [125] also leave altogether the impact of multidimensional vibrations in their analysis of a particle damper for wind turbines subjected to strong winds and gusts. They mention that the main mode is the most important and focus on damping that mode excited under free and forced vibrations around the peak of the natural frequency.

Table 3
Particle damping testing and modeling summary table, part 1 of 3.

Ref.	Exp./Sim.	Type	Freq. (Hz)	Ampl.	masses[a] (kg) of: structure; cavity; particle	particle diameter (mm)	packing fraction (%)	Comments
[109,110]	exp.	horizontal impact damper on brass tube	5–20	5 mm	1.37; -; 0.0076–0.0171	19.1	–	particle is an aluminum cylinder-like mass
[11]	both	impact damper inside and along tube	672[d]	2.4 mm	0.8[b]; -; 0.32	5 × 2	–	cylindrical particle
[7]	both	longitudinal beam PD	up to 6400	10 N	2.925; −0.331; ~0.213–0.432	0.1–0.5	50–100	beam with transverse and longitudinal PDs
[39]	both	centrifugal PD	5–18.3	3400; 14,000; 36,000 N mm	-; -; -	3	30–90	–
[120]	both	cube PD	–	–	-; -;	0.5–4	90	particles of aluminum oxide, steel, and tungsten carbide
[5]	both	plate PD	30–60	0.2–1 N	0.567; 0.048C[c]; 0.048C[c]	2	0–90	steel spheres
[64]	both	layered beam with PD at tip	~0.75[d]	6 cm	~0.45; -; 0.03–0.13	2–6	~100	most of the structure's weight comes from an added mass at its tip to reduce frequency; partial vacuum in cavity
[20]	both	cantilever beam PD	52.6[d]	–	0.0089; 0.021; -	–	–	microgravity environment; not enough information on the damper
[46]	both	combined impact and PD	11–15	0.135 N,	~0.232; -; 0.033	10 and 0.1	low	equivalent mass of beam is 0.104 kg

[a] Reporting the mass of the structure without damper and the total cumulative masses of the cavit (y/ies) and particle(s) present in the system; a negative cavity mass indicates that it was created by taking out material from the original structure.
[b] Reporting the reduced mass of the structure.
[c] The value is multiplied by a constant $C \in [0,1[$ because article only gives mass of the complete PD at maximum fill capacity.
[d] Natural frequency of the beam.

Table 4
Particle damping testing and modeling summary table, part 2 of 3.

Ref.	Exp./Sim.	Type	Freq. (Hz)	Ampl.	masses[a] (kg) of: structure; cavity; particle	particle diameter (mm)	packing fraction (%)	Comments
[121]	exp.	free-free beam	~130 and ~350	0.5–10 g	725 g;-;220 g	10	~100	size reported here for rubber spheres filling empty beam; tests with 0.3 mm thick metal swarf filling also done
[114]	exp.	oil pan PD	51.2	–	1.095; 0.899; 0.76[c]	up to 2.6[b]	up to 100	given structure weight is for the oil pan alone; mention strong weight reduction possible with proper design iterations
[80]	both	rotating cantilever beam PD	0–18.3 (rot.), 16–17 (bend.)	6 mm	~$[253; 16.5; 6.7] \times 10^3$	2–4	~35–60[e]	the cavity weight shown was reduced by 5 g of removed material from the beam; both imposed rotation and beam natural frequencies are given
[115]	both	cantilever beam NOPD	~0–1000[f]	–	16.5; ~ −0.0112[d]; up to 0.0163	~0.3 and 1	35–90	model impact of gas-particle interactions; cavity seals not considered in reported weights
[106]	both	building tuned mass damper PD	1.5–3	–	19.2; 0.01; 0.182	6	27.5	–
[122]	both	controlled vacuum PD	0.25–2.5	up to 25 mm/s	1200; -;	3×1	–	cylindrical plastic particles; underpressures between 0.01 and 0.09 MPa; given mass is the complete vehicle mass used for the numerical study

[a] Reporting the mass of the structure without damper and the total cumulative masses of the cavit (y/ies) and particle(s) present in the system; a negative cavity mass indicates that it was created by taking out material from the original structure.
[b] Material is sand with average particle size of 0.3 mm, and 95% of the particles below 0.48 mm.
[c] This is the maximum amount of granular material that can be held by the cavity.
[d] Reporting the reduced mass of the structure.
[e] This is an overestimate because measured as the volume envelope occupied by the particles to the total cavity volume.
[f] Studies the response covering the first four natural frequencies of the beam.

Table 5
Particle damping testing and modeling summary table, part 3 of 3.

Ref.	Exp./Sim.	Type	Freq. (Hz)	Ampl.	masses[a] (kg) of: structure; cavity; particle	particle diameter (mm)	packing fraction (%)	Comments
[8]	both	hollow particles PD on cantilever beam	100–1000	10–60 m/s^2	-; -;	–	50–100	–
[116]	exp.	particle-filled beam	impulse	from ~1000 to 35 600 N	273.8; 276.9; 90.8	~1[$]	0–100[b]	beam boundaries are steel plates and is suspended by bungee cords
[14]	exp.	cantilever beam and antenna PD	21 and 31	–	-; -; 0–0.136	3[c]	–	tests by releasing tensioned antenna
[44]	both	vacuum particle damper cantilevered beam	1.0–2.4	170 mm[d]	~1.46; ~1.29;	1 × 3	100[b]	cylindrical particles with length to diameter ratio ~3; underpressures from 0.01 MPa to 0.08 MPa
[17]	both	cantilever beam PD	0–500	–	0.118; 0.036; 0.007	2	16–39	beam identified at given frequency range and damper tested under free vibration initially excited at resonance
[9]	both	multi-unit particle damper	20–2000	8.1 g	7.47; up to 0.232[e]; -[e]	~0.85 and ~2	0–90[b]	test both lead spheres and tungsten powder separately

[$] Sizes of the particles used are not explicitly given and this is thus a crude estimate of the size of their polyethylene beads.
[a] Reporting the mass of the structure without damper and the total cumulative masses of the cavit (y/ies) and particle(s) present in the system; a negative cavity mass indicates that it was created by taking out material from the original structure.
[b] This is an overestimate because measured as the volume envelope occupied by the particles to the total cavity volume.
[c] Crude estimate of their particle dimensions from the given information.
[d] Maximum observed amplitude at vibration; caused by unbalance force of 0.287 kg at r = 3.7 cm.
[e] The weight is given as the maximum combined weight for 4 cavities and particles together.

Simonian and Brennan [126] test a particle damped beam which vibrates in both horizontal and vertical directions. They only report the results for the tests in the vertical direction. They find that the damper is mostly insensitive to excitation frequency. In a later publication, Simonian and Brennan [127] report that the damping they obtain with a particle damper on a cantilever beam is greater when shaking in the direction of gravity.

Windows-Yule et al. [128] report that two identical granular beds subjected to excitation forces of the same energy, but with different amplitudes and frequencies, may lead to very different energy contents inside their particles. Similarly, excitation with different energy contents may lead to quite similar particle energy contents. They use the particle-bed flight time to estimate the resonance frequency of the optimally damped system. For a column of particles, the flight time is calculated from the particle-particle coefficient of restitution, the cavity's base peak velocity, the number of particles N, and an empirical parameter. The equation does not hold when N is large and CoR is low because the energy gets instantly dissipated and frequency becomes less important. Thus, the findings of Windows-Yule et al. [128] concerning energy content may indicate that excitation in directions other than the principal one could lead to unexpected responses. However, their statement about energy being instantly dissipated when N is large may indicate that, for particle dampers with enough particles, parasitic vibrations may be negligible.

Finally, the literature indicates that the response of a particle damper is affected by the presence of lateral vibrations. When of equal phase, magnitude, and frequency, the effects of a perpendicular vibration may be similar to a rotation of the direction of excitation. As far as the authors are aware, no study focused on the impact of parasitic vibrations on the efficiency of the particle damper. However, the general approach seen in the literature is to consider them as harmless. This is confirmed by their use in wind turbines [125] and liquid oxygen shuttle engines [124] which are subjected to variable hydrodynamic loads with random amplitudes and frequencies in multiple directions other than the target vibration attenuation. It should also be noted that parasitic vibrations may have major negative impacts on the performance for dampers which rely on the state of matter of the granular material. Effectively, a small parasitic disturbance may, for example, cause a jamming transition or change the state of the granular material from solid-like to fluid- or gas-like. Nonetheless, testing with DEM presents the possibility to further verify this hypothesis.

6. Discussion

This literature survey gave an overview of particle damper design in its different forms. Aspects of modeling, using both lightweight analytical and heavier numerical formulations were presented. Trends regarding the efficiency of these dampers and impacts of different geometric and material parameters were also covered. Furthermore, optimization methods, model calibration, and experimental configurations were reported. Drawing from the information presented by this review, this section suggests a methodology for setting up numerical and experimental studies of particle-damped vibrating beams.

6.1. Numerical modeling

A dynamic model that simulates individual particles can work regardless of the nonlinearities pointed out by most authors. Consequently, it is recommended to rely on the DEM for the simulations. It also turns out to be the most popular approach for particle damper modeling.

It would be impractical and unnecessary to design a DEM algorithm from scratch. It is rather suggested to rely on one of the existing software. It should be chosen by comparing the constraints of the specific project to the capabilities of the software. For industrial projects, any code that provides the desired capabilities should do. For research projects, it is suggested to rely on open source codes because they provide extensive control over the contact laws. Both LIGGGHTS and Yade open source codes have been used for particle damper studies. Another open source toolkit to consider is Chrono. It properly reproduces standard experiments of granular material; it models flexible elements through FEM; it works in parallel; it offers two different DEM approaches; and, it is a multibody dynamics engine. A selective reading of the user manuals and, where possible, code of these toolkits is necessary to fully understand their potential. The choice should then be confirmed through benchmarking, calibration, and validation against experimental data or simulation with other codes. Individual assessment of the target application and corresponding tests should be made by the reader.

Usually, DEM software allows choosing the time step, the integration scheme, the contact model, the particle shape, the solution tolerance, the material parameters, and the initial conditions. These parameters are thus to be carefully chosen regardless of the chosen toolkit. For example, an explicit time-marching solution using a linear contact model should provide enough accuracy. However, in other cases the Hertz-type contact may be necessary for an improved solution. The mode in which the contact history is preserved should also be carefully selected. Although not necessary, relying on velocity-dependent coefficients of restitution, simulating presliding friction separately, or calculating the aerodynamic contribution of the containing fluid may provide more accurate modeling.

To speedup computer calculation time, the following can also be considered: attempt particle or cavity scaling; couple micro- and macro-scaling; opt for efficient contact detection algorithms; model using the maximum ratio of particle size to cavity size which yields constant results; artificially increase stiffness; reduce excitation velocities; or, use a single lumped particle, a single row or column, or a plane of particles instead of the complete particle bed. Nevertheless, great care should be taken to ensure such simplifications remain valid for the whole range of conditions for which they are used. For example, the minimization algorithm of the parameter identification or design optimization process could run with a simplified model and be verified with the original and slower model.

6.2. Remarks specific to DEM

Coupled methods improve the quality of the results but can considerably increase algorithm complexity and solution time. Solution time can be greatly reduced by employing a two-phase contact search algorithm. Contact detection algorithms do not perform with consistent speed and should thus be benchmarked for each new damper configuration.

The choice of the contact law is a challenging question and many authors choose to rely on bulk calibration to tune it. This allows to skip experimental testing of the single particles and consequently reduces the time to project completion. Tangential contact forces are another challenge and they are usually grossly estimated due to a lack of proper analytical formulations for tridimensional stick-slip alternating contact friction. Using rolling friction to tune the contact model is often used. However, it is also strongly criticized because of its lack of physical justification and its vulnerability when the configuration changes. The coefficients of friction and of restitution used for a DEM model can be significantly far from an exact value without affecting the measured damping efficiency of an optimally configured particle damper. Some authors obtained improved results without excessive effort when using velocity-dependent CoR. To summarize, contact model assumptions can be significantly far from the reality and still properly model the performance of the particle damper. But, these assumptions significantly increase the risk of completely ignoring important nonlinear behaviors such as phase changes when modeling outside of the experimentally tested range or outside of the optimal damper operation's range.

The choice of timestep is also an influential factor on computation speed. Many interpretation of a proper timestep exist and they also depend on the integration method used. For general DEM, it is, however, advisable that the zone between the coming into contact and departure times be sufficiently resolved. Diverse choices of timestep calculations are given in Section 4.5. Integration of the DEM equations is done with explicit schemes and the choice of scheme is usually done according to the preferences of the individual authors. Relying on already existing software allows for faster project completion and is the most popular choice. Whether to use open-source or commercial software should depend on the programming background of the researcher and the balance between funds and time resources. A look at Table 1 can give a first impression of the available software capabilities.

The identification of the DEM model parameters is highly variable between the studies. The principal outcome of this review is that three possibilities exist. 1) The parameters come directly from the literature: this will work when the purpose of the study is only to obtain the optimal damping performance that can be provided by the damper. 2) The parameters are bulk-calibrated: this can work when a considerable range of experiments are run to ensure that no unforeseen linear effects contradict the model. 3) The parameters are experimentally measured on individual particles and then bulk-calibrated: this will be the most tedious approach but will also provide the most reliable results.

Overall, DEM models a highly nonlinear phenomenon and relies on many material-based parameters. This leads to an apparently easy model setup and calibration that is, however, only able to reproduce already known results. Blind testing may be the only approach to overcome this paradox.

6.3. Identification

This survey showed that force models and the coefficients used therein significantly change from one study to the other. This indicates that the range of validity of each simulation is limited to the proper case. In addition, there is a discrepancy as to which parameters most influence the resulting damping. Some authors report that the coefficient of restitution is the main contributor while others opt for the coefficient of friction. Furthermore some terms, such as packing fraction, have inconsistent and ambiguous definitions in the literature.

Bulk calibration used alone is the prevalent approach for parameter identification and can thus be considered as reliable. However, to increase the range of validity of the obtained models, it is suggested to first build the DEM simulation using coefficients from the literature on materials. Optionally, simple experiments can also then identify the missing values. Then, a bulk calibration can tune the model to the experimental particle damper. While doing so, significantly varied test conditions should be used and the parameters should remain close to their literature values. Optimization algorithms which do not require the gradient of the objective function should be used as they are more likely to find a global optimum. Using the fit with position or velocity hysteresis loops, transmitted forces, energy dissipated, or particles trajectories as objective functions is suggested. Doing so will yield a model that is more robust given the nonlinearity of the response and valid over a greater range of conditions.

Also, assumptions about linear behavior should be made with great care as their validity may be restricted to specific ranges of parameters or operating conditions. Thus, conducting a sensitivity analysis both numerically and experimentally would assess the accuracy of the numerical method when testing conditions outside of the experimentally validated scope. The sensitivity study should identify the zones of operation where the model can be considered valid and whether parameters which are apparently non-influent can be activated by changes in other parameters. Finally, the model ran with the obtained parameters should be confronted with data from an experimental test using condition as different as possible from the bulk tests.

6.4. Experiments

To ensure the validity of the developed simulation approach, the identification process should be based on experimental data. An experiment is also recommended to calibrate and validate the numerical simulation. Both the experiments for identification

and for validation can be set up with similar compositions, but they should have operating conditions which are as different as possible from each other.

A particle damper mounted either directly on a shaker or on an excited beam, depending on the desired levels of accuracy and complexity, is suggested. Also, care should be taken to avoid over-constraining the structure; each test should be repeated 3 to 6 times to reduce statistical errors; the position where the beam is excited should be consistent between the different tests; and, inertial effects should be catered for by the identification model. Furthermore, the direction of the damper with respect to that of gravity and centrifugal forces should be carefully selected. Effectively, steady external pressure influences the initial settling of the particles in the cavity, the direction in which the impacts occur, and the forcing conditions at which phase transitions occur. The experimental forcing can be a displacement-induced free vibration, a sine sweep, an impulse, or a constant harmonic. It is recalled that granular material behaves in a highly nonlinear manner. Thus, a careful assessment of the operating environment of the target device should be made when choosing the type and magnitude of the experimental forcing. Also, it may be sound to test under supplementary vibration conditions to identify possible unforeseen behaviors such as phase transitions and jamming. These supplementary conditions should cover, at the very least, a range of frequencies near the fundamental mode. Furthermore, simulations should be run to identify the possible system responses and optimal operation ranges prior to choosing the details of the experimental campaign. Although not critical, if the experimental cavity is transparent or open on the upper side a high-speed video capture can provide further validation.

6.5. Damper performance

Multiple damping mechanisms were presented in this review and many of them were arguably quite effective at damping the vibrations targeted by the authors. Accordingly, a few notes on performance are given here.

Better performance occurs when the damper is placed away from the nodes of the mode shapes. That means better damping occurs when the damper is subjected to greater vibrations. Single particle impact dampers tend to be less efficient than granular dampers. That may, however, be linked to their necessity to be tuned. The energy content of the imposed vibration is not imperatively a driving factor on performance. However, it may change the dissipation mechanism of the particle damper.

The mass and packing ratios and clearance of particle dampers are always important, but it is not always clear how they influence performance. Their influence is linked to the properties of the applied forcing vibrations and more material does not necessarily mean a better damper. Usually, the best solution will come from a balance between allowing particle motion and not having excessive particle travel time. The type of particles used can change in shape, size, coefficient of restitution, and material without necessarily influencing the damping efficiency. Effectively, these parameters may influence the motion of the granular bed without having a significant impact on dissipation. The changes should, however, remain within boundaries that become known from simulation or experiment. For particle dampers, longer cavities bored inside the structure stimulate shear friction and consequently improve damping. As such, shape, aspect ratio, and the number of cavities influences performance. This influence depends on the properties of the forcing vibration.

Simultaneous and synchronized excitation in multiple directions can influence performance as if the damper were rotated and subjected to an equivalently larger force. This holds when nonlinear effects do not dominate. An abundantly filled damper cavity may mitigate parasitic vibrations in secondary directions and promote damping by favoring rolling friction. Vibration of the particle damper in the horizontal direction can improve damping by stimulating oblique impacts but this is not always true. For vertically vibrating dampers, acceleration must overcome gravity for the granules to reach the top of the cavity. Combining a large particle such as that of an impact damper with fine granular material can improve the damping performance of the resulting damper. This is likely due to the resulting condition in which the large particle finds itself which mimics the Leidenfrost effect and biconvective state. Non-rigid material at the cavity walls can improve performance. Similarly, actively controlled walls can influence the phase state of the particles and further increase the damping capacity. Accordingly, the granular material provides the best performance when being at the edge of transitioning to a fluid-like state.

6.6. Design considerations

Various particle damper typologies are presented in this survey: damper excited in oblique or two directions; multi-unit dampers; non-obstructive dampers; tuned mass particle dampers; differential particle sizes; vacuum dampers and other active solutions; and, combined particles of different materials and shapes. For vibrating beams, the non-obstructive damper with a uniform particle size may be the most lightweight and efficient damping solution. The cavity should be positioned at the location of maximum response amplitude, as this is repeatedly mentioned in the literature. The use of soft material on the cavity walls may improve effectiveness. In that case, the chosen material should withstand the environmental exposure that could affect the efficiency of the damping. With a properly tuned DEM simulation, it is possible to identify whether most energy dissipation comes from particle-wall or particle-particle friction or impact and thus indicate possible modifications for improved damping. Finally, care should be taken to avoid possible detrimental behavior of the damper. For example, there may be excitation patterns for which the damper increases the amplitude of the vibration. In its most extreme occurrence, this eventuality could be compared to the rogue wave phenomenon, which is rare but very dangerous.

7. Conclusion

This survey provided an overview of modeling and testing particle dampers used on beams. A glimpse of research opportunities based on the current the state of the art is given and followed by a closing word.

7.1. Opportunities for further research

From the reviewed literature, it appears that remaining open questions present good opportunities to conduct further research. The authors believe that future research should focus on: the effect of parasitic vibrations; the importance of gravity, centrifugal forces, and actively applied pressure; the influence of cavity material; the definition of standardized granular bed phase states; the use of implicit numerical particle solvers, and, the establishment of consistent DEM modeling schemes and parameter choices.

7.2. Closing word

Particle dampers were seen to be the central point of a numerous number of studies, of which only a small fraction was presented here. They present appealing dissipation properties and can be used in harsh environments. This paper presented a global overview of their use, advantages, modeling techniques, design considerations, and experimental testing. The interested reader may also consult the review on particle dampers for civil engineering applications by Lu et al. [12], the Discrete Element Method book by Matuttis and Chen [54], and the vibration and impact dynamics book by Ibrahim [3].

Acknowledgments

This paper was funded by the European Community's Horizon 2020 Programme (H2020-EU.3.4.5.5. - ITD Engines) under grant agreement N. 687023 (EMS UHPE - Engine Mount System for Ultra High Pass Engine).

References

[1] S.F. Masri, A.M. Ibrahim, Response of the impact damper to stationary random excitation, J. Acoust. Soc. Am. 53 (1) (1973) 200–211, https://doi.org/10.1121/1.1913319.
[2] C. Saluea, T. Pschel, S.E. Esipov, Dissipative properties of vibrated granular materials, Phys. Rev. E, ISSN: 1063-651X 59 (4) (1999) 4422–4425, https://doi.org/10.1103/PhysRevE.59.4422 1095-3787.
[3] R. Ibrahim, Vibro-impact Dynamics: Modeling, Mapping and Applications, vol. 43, Springer-Verlag Berlin Heidelberg, 2009.
[4] Z. Lu, Z. Wang, S.F. Masri, X. Lu, Particle impact dampers: past, present, and future, Struct. Control Health Monit. 25 (1) (2017) e2058, https://doi.org/10.1002/stc.2058.
[5] Z. Xia, X. Liu, Y. Shan, X. Li, Coupling simulation algorithm of discrete element method and finite element method for particle damper, J. Low Freq. Noise Vib. Act. Control 28 (3) (2009) 197–204, https://doi.org/10.1260/026309209790252545.
[6] Z. Lu, X. Lu, H. Jiang, S.F. Masri, Discrete element method simulation and experimental validation of particle damper system, Eng. Comput. 31 (4) (2014) 810–823, https://doi.org/10.1108/EC-08-2012-0191.
[7] Z. Xu, M.Y. Wang, T. Chen, Particle damping for passive vibration suppression: numerical modelling and experimental investigation, J. Sound Vib., ISSN: 0022-460X 279 (3) (2005) 1097–1120. https://doi.org/10.1016/j.jsv.2003.11.023.
[8] G. Michon, A. Almajid, G. Aridon, Soft hollow particle damping identification in honeycomb structures, J. Sound Vib., ISSN: 0022-460X 332 (3) (2013) 536–544. https://doi.org/10.1016/j.jsv.2012.09.024.
[9] X. Wang, X. Liu, Y. Shan, T. He, Design, simulation and experiment of particle dampers attached to a precision instrument in spacecraft, J. Vibroeng. 17 (4) (2015) 1605–1614. www.scopus.com. cited By:2.
[10] M. Snchez, C.M. Carlevaro, L.A. Pugnaloni, Effect of particle shape and fragmentation on the response of particle dampers, J. Vib. Control 20 (12) (2014) 1846–1854, https://doi.org/10.1177/1077546313480544.
[11] A. Oldzki, I. Siwicki, J. Winiewski, Impact dampers in application for tube, rod and rope structures, Mech. Mach. Theory 34 (2) (1999) 243–253, https://doi.org/10.1016/s0094-114x(98)00014-7.
[12] Z. Lu, X. Chen, Y. Zhou, An equivalent method for optimization of particle tuned mass damper based on experimental parametric study, J. Sound Vib., ISSN: 0022-460X 419 (2018) 571–584. https://doi.org/10.1016/j.jsv.2017.05.048.
[13] Z. Lu, S.F. Masri, X. Lu, Studies of the performance of particle dampers attached to a two-degrees-of-freedom system under random excitation, J. Vib. Control 17 (10) (2011) 1454–1471, https://doi.org/10.1177/1077546310370687.
[14] S.S. Simonian, Particle beam damper, in: Proc. SPIE, vol. 2445, 1995, https://doi.org/10.1117/12.208884. 2445 2445 12.
[15] D.I. Suyama, A.E. Diniz, R. Pederiva, The use of carbide and particle-damped bars to increase tool overhang in the internal turning of hardened steel, Int. J. Adv. Manuf. Technol., ISSN: 1433-3015 86 (5) (2016) 2083–2092, https://doi.org/10.1007/s00170-015-8328-z.
[16] A. Papalou, S.F. Masri, Response of impact dampers with granular materials under random excitation, Earthq. Eng. Struct. Dyn. 25 (3) (1996) 253–267, https://doi.org/10.1002/(SICI)1096-9845(199603)25:3<253::AID-EQE553>3.0.CO;2-4.
[17] M. Trigui, E. Foltete, M.S. Abbes, T. Fakhfakh, N. Bouhaddi, M. Haddar, An experimental study of a multi-particle impact damper, Proc. Inst. Mech. Eng. C J. Mech. Eng. Sci. 223 (9) (2009) 2029–2038, https://doi.org/10.1243/09544062jmes1400.
[18] S.E.O. Bryce, L. Fowler, Eric M. Flint, Effectiveness and predictability of particle damping, in: Proceedings Volume 3989, Smart Structures and Materials 2000: Damping and Isolation, vol. 3989, 2000, https://doi.org/10.1117/12.384576. 3989 3989 12.
[19] C. Wong, M. Daniel, J. Rongong, Energy dissipation prediction of particle dampers, J. Sound Vib., ISSN: 0022-460X 319 (1) (2009) 91–118. https://doi.org/10.1016/j.jsv.2008.06.027.
[20] J.L. Brown, A Space Based Particle Damper Demonstrator, Master's Thesis, California Polytechnic State University, San Luis Obispo, California, 2011.
[21] M. Snchez, G. Rosenthal, L.A. Pugnaloni, Universal response of optimal granular damping devices, J. Sound Vib., ISSN: 0022-460X 331 (20) (2012) 4389–4394. https://doi.org/10.1016/j.jsv.2012.05.001.
[22] G.H. Ristow, Critical exponents for granular phase transitions, Europhys. Lett. (EPL), ISSN: 0295-5075 40 (6) (1997) 625–630, https://doi.org/10.1209/epl/i1997-00514-3. 1286-4854 arXiv:cond-mat/9706168.

[23] K. Zhang, T. Chen, X. Wang, J. Fang, Motion mode of the optimal damping particle in particle dampers, J. Mech. Sci. Technol., ISSN: 1976-3824 30 (4) (2016) 1527–1531, https://doi.org/10.1007/s12206-016-0305-4.
[24] E. DeGiuli, J.N. McElwaine, M. Wyart, Phase diagram for inertial granular flows, Phys. Rev. E, ISSN: 2470-0045 94 (1) (2016) 012904, https://doi.org/10.1103/PhysRevE.94.012904. 2470-0053 http://arxiv.org/abs/1509.03512.
[25] F. Pacheco-Vzquez, F. Ludewig, S. Dorbolo, Dynamics of a grain-filled ball on a vibrating plate, Phys. Rev. Lett. 113 (11) (2014) 118001, https://doi.org/10.1103/PhysRevLett.113.118001.
[26] K. Zhang, T. Chen, L. He, Damping behaviors of granular particles in a vertically vibrated closed container, Powder Technol., ISSN: 0032-5910 321 (2017) 173–179, https://doi.org/10.1016/j.powtec.2017.08.020.
[27] M.E. Cates, J. Wittmer, J.P. Bouchaud, P. Claudin, Jamming, force chains and fragile matter, Phys. Rev. Lett., ISSN: 0031-9007 81 (9) (1998) 1841–1844, https://doi.org/10.1103/PhysRevLett.81.1841. 1079-7114 arXiv:cond-mat/9803197.
[28] J. Rongong, G. Tomlinson, Amplitude dependent behaviour in the application of particle dampers to vibrating structures, in: 46th AIAA/ASME/ASCE/AHS/ASC Structures, Structural Dynamics and Materials Conference, Structures, Structural Dynamics, and Materials and Co-located Conferences, American Institute of Aeronautics and Astronautics, 2005, https://doi.org/10.2514/6.2005-2327.
[29] C. Wong, J. Rongong, Control of particle damper nonlinearity, AIAA J., ISSN: 0001-1452 47 (4) (2009) 953–960, https://doi.org/10.2514/1.38795.
[30] J.M. Bajkowski, B. Dyniewicz, M. Gbik-Wrona, J. Bajkowski, C.I. Bajer, Reduction of the vibration amplitudes of a harmonically excited sandwich beam with controllable core, Mech. Syst. Signal Process., ISSN: 0888-3270 129 (2019) 54–69. https://doi.org/10.1016/j.ymssp.2019.04.024.
[31] J.M. Bajkowski, B. Dyniewicz, C.I. Bajer, Semi-active damping strategy for beams system with pneumatically controlled granular structure, Mech. Syst. Signal Process., ISSN: 0888-3270 7071 (2016) 387–396, https://doi.org/10.1016/j.ymssp.2015.09.026.
[32] J.M. Bajkowski, C. Bajer, B. Dyniewicz, D. Pisarski, Vibration control of adjacent beams with pneumatic granular coupler: an experimental study, Mech. Res. Commun., ISSN: 0093-6413 78 (2016) 51–56. https://doi.org/10.1016/j.mechrescom.2016.10.005.
[33] G. Kuwabara, K. Kono, Restitution coefficient in a collision between two spheres, Jpn. J. Appl. Phys. 26 (8R) (1987) 1230. http://stacks.iop.org/1347-4065/26/i8R/a1230 eqn. 7.
[34] M.E. Fayed, L. Otten (Eds.), Handbook of Powder Science & Technology, second ed., Springer US, 1997, https://doi.org/10.1007/978-1-4615-6373-0.
[35] K.-H. Leitz, M. O'Sullivan, A. Plankensteiner, H. Kestler, L.S. Sigl, OpenFOAM modeling of particle heating and acceleration in cold spraying, J. Therm. Spray Technol., ISSN: 1544-1016 27 (1) (2018) 135–144, https://doi.org/10.1007/s11666-017-0644-4.
[36] S. Dissanayake, S. Karunarathne, J. Lundberg, L.-A. Tokheim, CFD study of particle flow patterns in a rotating cylinder applying OpenFOAM and fluent, in: Proceedings of the 58th SIMS, Linkping University Electronic Press, 2017, https://doi.org/10.3384/ecp17138137.
[37] P.J. O'Rourke, P.P. Zhao, D. Snider, A model for collisional exchange in gas/liquid/solid fluidized beds, Chem. Eng. Sci., ISSN: 0009-2509 64 (8) (2009) 1784–1797. https://doi.org/10.1016/j.ces.2008.12.014.
[38] W. Xiao, Z. Chen, T. Pan, J. Li, Research on the impact of surface properties of particle on damping effect in gear transmission under high speed and heavy load, Mech. Syst. Signal Process., ISSN: 0888-3270 98 (2018) 1116–1131. https://doi.org/10.1016/j.ymssp.2017.05.021.
[39] W. Xiao, Y. Huang, H. Jiang, H. Lin, J. Li, Energy dissipation mechanism and experiment of particle dampers for gear transmission under centrifugal loads, Particuology, ISSN: 1674-2001 27 (2016) 40–50. https://doi.org/10.1016/j.partic.2015.10.007.
[40] B. Brogliato, Nonsmooth Impact Mechanics, Springer-Verlag, 1996, https://doi.org/10.1007/bfb0027733.
[41] X. Fang, H. Luo, J. Tang, Investigation of granular damping in transient vibrations using Hilbert Transform based technique, J. Vib. Acoust. 130 (3) (2008) 031006, https://doi.org/10.1115/1.2827454.
[42] B. Brogliato, Nonsmooth Mechanics: Models, Dynamics and Control, Springer International Publishing, 2016, https://doi.org/10.1007/978-3-319-28664-8.
[43] M. Saeki, Analytical study of multi-particle damping, J. Sound Vib. 281 (35) (2005) 1133–1144, https://doi.org/10.1016/j.jsv.2004.02.034. cited By 97.
[44] T. Szmidt, R. Zalewski, Inertially excited beam vibrations damped by Vacuum Packed Particles, Smart Mater. Struct. 23 (10) (2014) 105026, https://doi.org/10.1088/0964-1726/23/10/105026.
[45] J. Park, D.L. Palumbo, Damping of structural vibration using lightweight granular materials, Exp. Mech., ISSN: 1741-2765 49 (5) (2009) 697–705, https://doi.org/10.1007/s11340-008-9181-x.
[46] Y. Du, S. Wang, Modeling the fine particle impact damper, Int. J. Mech. Sci., ISSN: 0020-7403 52 (7) (2010) 1015–1022. https://doi.org/10.1016/j.ijmecsci.2010.04.004.
[47] I. Yokomichi, Y. Araki, Y. Jinnouchi, J. Inoue, Impact damper with granular materials for multibody system, J. Press. Vessel Technol. 118 (1) (1996) 95, https://doi.org/10.1115/1.2842169.
[48] K. Iglberger, U. Rde, The Pe Rigid Multibody Physics Engine, Tech. Rep., Friedrich-Alexander University of Erlangen-Nuremberg, 2009.
[49] K. Iglberger, U. Rde, Massively parallel rigid body dynamics simulations, Comput. Sci. Res. Dev. 23 (34) (2009) 159–167, https://doi.org/10.1007/s00450-009-0066-8.
[50] H. Elmqvist, A. Goteman, V. Roxling, T. Ghandriz, Generic modelica framework for MultiBody contacts and discrete element method, in: Proceedings of the 11th International Modelica Conference, Versailles, France, September 21-23, 2015, Linkping University Electronic Press, 2015, https://doi.org/10.3384/ecp15118427.
[51] P.A. Cundall, O.D.L. Strack, A discrete numerical model for granular assemblies, Geotechnique 29 (1) (1979) 47–65, https://doi.org/10.1680/geot.1979.29.1.47.
[52] R. Ehrgott, H. Panossian, G. Davis, Modeling Techniques for Evaluating the Effectiveness of Particle Damping in Turbomachinery, Tech. Rep. MSFC-2224, NASA, 2009.
[53] M. Saeki, Impact damping with granular materials in a horizontally vibrating system, J. Sound Vib. 251 (1) (2002) 153–161, https://doi.org/10.1006/jsvi.2001.3985. cited By 118.
[54] H.-G. Matuttis, J. Chen, Understanding the Discrete Element Method, John Wiley & Sons (Asia) Pte. Ltd, 2014, https://doi.org/10.1002/9781118567210.
[55] M. Kwarta, D. Negrut, Using the Complementarity and Penalty Methods for Solving Frictional Contact Problems in Chrono: Validation for the Cone Penetration Test, Tech. Rep. TR-2016-16, University of Wisconsin-Madison, 2017.
[56] Y. Wang, B. Liu, A. Tian, W. Tang, Experimental and numerical investigations on the performance of particle dampers attached to a primary structure undergoing free vibration in the horizontal and vertical directions, J. Sound Vib., ISSN: 0022-460X 371 (2016) 35–55. https://doi.org/10.1016/j.jsv.2016.01.056.
[57] Y. Duan, Q. Chen, Simulation and experimental investigation on dissipative properties of particle dampers, J. Vib. Control 17 (5) (2011) 777–788, https://doi.org/10.1177/1077546309356183.
[58] P. Klinge, SIMPRO/VTT Task 2.3 - Optimisation of a Particle Damper with DEM, Tech. Rep. VTT-R-00651-14, Tekes - Finnish Funding Agency For Technology And Innovation, 2015.
[59] P. Chodkiewicz, J. Lengiewicz, R. Zalewski, Discrete element method approach to modelling VPP dampers, in: MATEC Web of Conferences, vol. 157, 2018, https://doi.org/10.1051/matecconf/201815702014. cited By 0.
[60] M. Masmoudi, S. Job, M.S. Abbes, I. Tawfiq, M. Haddar, Experimental and numerical investigations of dissipation mechanisms in particle dampers, Granul. Matter, ISSN: 1434-7636 18 (3) (2016) 71, https://doi.org/10.1007/s10035-016-0667-4.
[61] M. Snchez, C.M. Carlevaro, Nonlinear dynamic analysis of an optimal particle damper, J. Sound Vib., ISSN: 0022-460X 332 (8) (2013) 2070–2080. https://doi.org/10.1016/j.jsv.2012.09.042.
[62] M. Snchez, L.A. Pugnaloni, Effective mass overshoot in single degree of freedom mechanical systems with a particle damper, J. Sound Vib., ISSN: 0022-460X 330 (24) (2011) 5812–5819. https://doi.org/10.1016/j.jsv.2011.07.016.
[63] C. Coetzee, Review: calibration of the discrete element method, Powder Technol., ISSN: 0032-5910 310 (2017) 104–142. https://doi.org/10.1016/j.powtec.2017.01.015.

[64] J.M. Bajkowski, B. Dyniewicz, C.I. Bajer, Damping properties of a beam with vacuum-packed granular damper, J. Sound Vib., ISSN: 0022-460X 341 (2015) 74–85. https://doi.org/10.1016/j.jsv.2014.12.036.

[65] R. Zalewski, P. Chodkiewicz, Semi-active linear vacuum packed particles damper, J. Theor. Appl. Mech. (2016) 311, https://doi.org/10.15632/jtam-pl.54.1.311.

[66] E.M. Campello, A computational model for the simulation of dry granular materials, Int. J. Non-Linear Mech., ISSN: 0020-7462 106 (2018) 89–107. https://doi.org/10.1016/j.ijnonlinmec.2018.08.010.

[67] C. O'Sullivan, Developing robust DEM models to simulate element tests, in: Presentation for the Doctoral School of the GEO-RAMP Project, from PDF-Rendered Presentation, 2016.

[68] A. Rousset, A.W.M. Checkaraou, Y.-C. Liao, X. Besseron, S. Varrette, B. Peters, Comparing broad-phase interaction detection algorithms for multiphysics DEM applications, AIP Conf. Proceed. 1978 (1) (2018) 270007, https://doi.org/10.1063/1.5043900.

[69] M. Lin, S. Gottschalk, Collision detection between geometric models: a survey, in: Proc. of IMA Conference on Mathematics of Surfaces, vol. 1, 1998, pp. 602–608.

[70] A. Brintaki, S.K. Lai-Yuen, eBGF: an enhanced geometric hierarchical representation for protein modeling and rapid self-collision detection, Comput.-Aided Design Appl. 6 (2009) 625–638, https://doi.org/10.3722/cadaps.2009.625-638.

[71] S. Dinas, J.M. Banon, A literature review of bounding volumes hierarchy focused on collision detection, Ing. Competitividad, ISSN: 0123-3033 17 (2015) 49–62.

[72] J.J. Jimnez, R.J. Segura, Collision detection between complex polyhedra, Comput. Graph., ISSN: 0097-8493 32 (4) (2008) 402–411. https://doi.org/10.1016/j.cag.2008.05.002.

[73] G.S. Grest, B. Dnweg, K. Kremer, Vectorized link cell Fortran code for molecular dynamics simulations for a large number of particles, Comput. Phys. Commun., ISSN: 0010-4655 55 (3) (1989) 269–285. https://doi.org/10.1016/0010-4655(89)90125-2.

[74] J. Horabik, M. Molenda, Parameters and contact models for DEM simulations of agricultural granular materials: a review, Biosyst. Eng., ISSN: 1537-5110 147 (2016) 206–225. https://doi.org/10.1016/j.biosystemseng.2016.02.017.

[75] K. Mao, M.Y. Wang, Z. Xu, T. Chen, DEM simulation of particle damping, Powder Technol., ISSN: 0032-5910 142 (2) (2004) 154–165. https://doi.org/10.1016/j.powtec.2004.04.031.

[76] D.N.J. Els, Damping of rotating beams with particle dampers: discrete element method analysis, AIP Conf. Proceed. 1542 (1) (2013) 867–870, https://doi.org/10.1063/1.4812069.

[77] B. Darabi, Dissipation of Vibration Energy Using Viscoelastic Granular Materials. (Ph.D. thesis), University of Sheffield, 2013.

[78] S. Timoshenko, Theory of Elasticity, Engineering Societies Monographs, McGraw-Hill, 1951, https://books.google.it/books?idNlMSAAAAIAAJ. eq. 219.

[79] H. Hertz, Ueber die Berhrung fester elastischer Krper (About the contact of solid elastic bodies), J. fr die Reine Angewandte Math. 92 (1882) 156–171. http://eudml.org/doc/148490.

[80] D.N.J. Els, Damping of rotating beams with particle dampers: experimental analysis, AIAA J. 49 (10) (2011) 2228–2238, https://doi.org/10.2514/1.j050984.

[81] R.D. Mindlin, Elastic spheres in contact under varying oblique forces, J. Appl. Mech. 20 (1953) 327–344. https://ci.nii.ac.jp/naid/10014584853/en/.

[82] S. Liu, D. Sun, H. Matsuoka, On the interface friction in direct shear test, Comput. Geotech. 32 (5) (2005) 317–325, https://doi.org/10.1016/j.compgeo.2005.05.002.

[83] C. de Wit, P. Lischinsky, K. strm, H. Olsson, A new model for control of systems with friction, IEEE Trans. Autom. Control 40 (3) (1995) 419–425, https://doi.org/10.1109/9.376053. cited By 2220.

[84] J. Gong, J. Liu, Mechanical transitional behavior of binary mixtures via DEM: effect of differences in contact-type friction coefficients, Comput. Geotech., ISSN: 0266-352X 85 (2017) 1–14. https://doi.org/10.1016/j.compgeo.2016.12.009.

[85] Y. He, T. Evans, A. Yu, R. Yang, DEM investigation of the role of friction in mechanical response of powder compact, Powder Technol., ISSN: 0032-5910 319 (2017) 183–190. https://doi.org/10.1016/j.powtec.2017.06.055.

[86] P. Dupont, V. Hayward, B. Armstrong, F. Altpeter, Single state elastoplastic friction models, IEEE Trans. Autom. Control 47 (5) (2002) 787–792, https://doi.org/10.1109/TAC.2002.1000274. cited By 298.

[87] R. Baleviius, Z. Mrz, The combined slip and finite sliding models in a frictional contact interaction of two spherical particles, Procedia Eng., ISSN: 1877-7058 57 (2013) 167–174. https://doi.org/10.1016/j.proeng.2013.04.024 modern Building Materials, Structures and Techniques.

[88] H. Hayakawa, Simulation of granular friction and its effective theory, Prog. Theor. Phys. Suppl. 138 (2000) 537–542, https://doi.org/10.1143/PTPS.138.537.

[89] Z. Syed, M. Tekeste, D. White, A coupled sliding and rolling friction model for DEM calibration, J. Terramechanics, ISSN: 0022-4898 72 (2017) 9–20. https://doi.org/10.1016/j.jterra.2017.03.003.

[90] C. Wensrich, A. Katterfeld, Rolling friction as a technique for modelling particle shape in DEM, Powder Technol., ISSN: 0032-5910 217 (2012) 409–417. https://doi.org/10.1016/j.powtec.2011.10.057.

[91] M. Holmes, R. Brown, P. Wauters, N. Lavery, S. Brown, Bending and twisting friction models in soft-sphere discrete element simulations for static and dynamic problems, Appl. Math. Model. 40 (56) (2016) 3655–3670, https://doi.org/10.1016/j.apm.2015.10.026.

[92] D. Sohn, Y. Lee, M.-Y. Ahn, Y.-H. Park, S. Cho, Numerical prediction of packing behavior and thermal conductivity of pebble beds according to pebble size distributions and friction coefficients, Fusion Eng. Des., ISSN: 0920-3796 137 (2018) 182–190. https://doi.org/10.1016/j.fusengdes.2018.09.012.

[93] M. Machado, P. Moreira, P. Flores, H.M. Lankarani, Compliant contact force models in multibody dynamics: evolution of the Hertz contact theory, Mech. Mach. Theory, ISSN: 0094-114X 53 (2012) 99–121. https://doi.org/10.1016/j.mechmachtheory.2012.02.010.

[94] B. Suhr, K. Six, Friction phenomena and their impact on the shear behaviour of granular material, Comput. Particle Mech., ISSN: 2196-4386 4 (1) (2017) 23–34, https://doi.org/10.1007/s40571-016-0119-2.

[95] S. McNamara, E. Falcon, Simulations of vibrated granular medium with impact-velocity-dependent restitution coefficient, Phys. Rev. E 71 (2005) 031302https://doi.org/10.1103/PhysRevE.71.031302.

[96] Z. Lu, X. Lu, S.F. Masri, Studies of the performance of particle dampers under dynamic loads, J. Sound Vib., ISSN: 0022-460X 329 (26) (2010) 5415–5433. https://doi.org/10.1016/j.jsv.2010.06.027.

[97] J. Fleischmann, DEM-PM Contact Model with Multi-step Tangential Contact Displacement History, Tech. Rep. TR-2015-06, University of Wisconsin-Madison, 2015.

[98] H. Pourtavakoli, E.J.R. Parteli, T. Pschel, Granular dampers: does particle shape matter? New J. Phys. 18 (7) (2016) 073049, http://stacks.iop.org/1367-2630/18/i7/a073049.

[99] J. Kozicki, F. Donz, A new open-source software developed for numerical simulations using discrete modeling methods, Comput. Methods Appl. Mech. Eng., ISSN: 0045-7825 197 (49) (2008) 4429–4443. https://doi.org/10.1016/j.cma.2008.05.023.

[100] A. Tasora, R. Serban, H. Mazhar, A. Pazouki, D. Melanz, J. Fleischmann, M. Taylor, H. Sugiyama, D. Negrut, Chrono: an open source multi-physics dynamics engine, in: T. Kozubek, R. Blaheta, J. stek, M. Rozlonk, M. ermk (Eds.), High Performance Computing in Science and Engineering, Springer International Publishing, Cham, 2016, ISBN: 978-3-319-40361-8, pp. 19–49.

[101] T.-T. Ng, Input parameters of discrete element methods, J. Eng. Mech. 132 (7) (2006) 723–729, https://doi.org/10.1061/(ASCE)0733-9399(2006)132:7(723).

[102] D. Hastie, Experimental measurement of the coefficient of restitution of irregular shaped particles impacting on horizontal surfaces, Chem. Eng. Sci., ISSN: 0009-2509 101 (2013) 828–836. https://doi.org/10.1016/j.ces.2013.07.010.

[103] L. Zheng, L. Xilin, L. Wensheng, S.F. Masri, Shaking table test of the effects of multiunit particle dampers attached to an MDOF system under earthquake excitation, Earthq. Eng. Struct. Dyn. 41 (5) (2012) 987–1000, https://doi.org/10.1002/eqe.1170.

[104] Z. Lu, X. Lu, W. Lu, S.F. Masri, Experimental studies of the effects of buffered particle dampers attached to a multi-degree-of-freedom system under dynamic loads, J. Sound Vib., ISSN: 0022-460X 331 (9) (2012) 2007–2022. https://doi.org/10.1016/j.jsv.2011.12.022.

[105] K. Li, A. Darby, An experimental investigation into the use of a buffered impact damper, J. Sound Vib., ISSN: 0022-460X 291 (3) (2006) 844–860. https://doi.org/10.1016/j.jsv.2005.06.043.
[106] Z. Lu, D. Wang, S. Masri, X. Lu, An experimental study of vibration control of wind-excited high-rise buildings using particle tuned mass dampers, Smart Struct. Syst. 18 (1) (2016) 93–115.
[107] A. Stevens, C. Hrenya, Comparison of soft-sphere models to measurements of collision properties during normal impacts, Powder Technol., ISSN: 0032-5910 154 (2) (2005) 99–109. https://doi.org/10.1016/j.powtec.2005.04.033.
[108] A. Oldzki, A new kind of impact damperfrom simulation to real design, Mech. Mach. Theory, ISSN: 0094-114X 16 (3) (1981) 247–253, https://doi.org/10.1016/0094-114X(81)90039-2.
[109] F.A. Akl, A.S. Butt, Application of Impact Dampers in Vibration Control of Flexible Structures, Tech. Rep. N95- 32420, NASA, 1995.
[110] A.S. Butt, F.A. Akl, Experimental analysis of impact-damped flexible beams, J. Eng. Mech. 123 (4) (1997) 376–383, https://doi.org/10.1061/(asce)0733-9399(1997)123:4(376).
[111] R.D. Wildman, J.M. Huntley, H. Jean-Pierre, Experimental Studies of Vibro-Fluidised Granular Beds, Springer Berlin Heidelberg, Berlin, Heidelberg, 2001, pp. 215–232, https://doi.org/10.1007/3-540-44506-4_12.
[112] K.S. Marhadi, V.K. Kinra, Particle impact damping: effect of mass ratio, material, and shape, J. Sound Vib. 283 (12) (2005) 433–448, https://doi.org/10.1016/j.jsv.2004.04.013.
[113] R. Friend, V. Kinra, Particle impact damping, J. Sound Vib., ISSN: 0022-460X 233 (1) (2000) 93–118. https://doi.org/10.1006/jsvi.1999.2795.
[114] F. Duvigneau, S. Koch, E. Woschke, U. Gabbert, An effective vibration reduction concept for automotive applications based on granular-filled cavities, J. Vib. Control 24 (1) (2018) 73–82, https://doi.org/10.1177/1077546316632932.
[115] X. Lei, C. Wu, Non-obstructive particle damping using principles of gas-solid flows, J. Mech. Sci. Technol., ISSN: 1976-3824 31 (3) (2017) 1057–1065, https://doi.org/10.1007/s12206-017-0204-3.
[116] L.W. Salvino, P. Dupont, J.G. McDaniel, Evaluation of granular-fill damping in a shock-loaded box beam, in: Proceedings of the 69th Shock and Vibration Symposium, 1998.
[117] J. McDaniel, P. Dupont, L. Salvino, A wave approach to estimating frequency-dependent damping under transient loading, J. Sound Vib., ISSN: 0022-460X 231 (2) (2000) 433–449. https://doi.org/10.1006/jsvi.1999.2723.
[118] R. Zalewski, T. Szmidt, Application of Special Granular Structures for semi-active damping of lateral beam vibrations, Eng. Struct., ISSN: 0141-0296 65 (2014) 13–20. https://doi.org/10.1016/j.engstruct.2014.01.035.
[119] Y. Iwata, T. Komatsuzaki, S. Kitayama, T. Takasaki, Study on optimal impact damper using collision of vibrators, J. Sound Vib. 361 (2016) 66–77, https://doi.org/10.1016/j.jsv.2015.09.036.
[120] W.-Q. Xiao, W. Li, Collision energy dissipation calculation and experiment for impact damper with particles, Sensors Transducers 159 (2013) 442–449.
[121] H. Abbas, H. Hai, J. Rongong, Y. Xing, Damping performance of metal swarfs in a horizontal hollow structure, J. Mech. Sci. Technol., ISSN: 1976-3824 28 (1) (2014) 9–13, https://doi.org/10.1007/s12206-013-0980-3.
[122] M. Makowski, R. Zalewski, Vibration analysis for vehicle with vacuum packed particles suspension, J. Theor. Appl. Mech. 53 (2015) 109.
[123] S.O. Oyadiji, Damping of vibrations of hollow beams using viscoelastic spheres, in: C.D. Johnson (Ed.), Smart Structures and Materials 1996: Passive Damping and Isolation, SPIE, 1996https://doi.org/10.1117/12.239078.
[124] H.V. Panossian, Structural damping enhancement via non-obstructive particle damping technique, J. Vib. Acoust. 114 (1) (1992) 101, https://doi.org/10.1115/1.2930221.
[125] J. Chen, C.T. Georgakis, Tuned rolling-ball dampers for vibration control in wind turbines, J. Sound Vib., ISSN: 0022-460X 332 (21) (2013) 5271–5282. https://doi.org/10.1016/j.jsv.2013.05.019.
[126] S.S. Simonian, S. Brennan, New particle damping applications, in: Collection of Technical Papers - AIAA/ASME/ASCE/AHS/ASC Structures, Structural Dynamics and Materials Conference, vol. 10, 2006, pp. 7314–7326.
[127] S.S. Simonian, S. Brennan, Parametric test results on particle dampers, in: Collection of Technical Papers - AIAA/ASME/ASCE/AHS/ASC Structures, Structural Dynamics and Materials Conference, vol. 4, 2007, pp. 4192–4208.
[128] C.R.K. Windows-Yule, A.D. Rosato, A.R. Thornton, D.J. Parker, Resonance effects on the dynamics of dense granular beds: achieving optimal energy transfer in vibrated granular systems, New J. Phys. 17 (2) (2015) 023015, http://stacks.iop.org/1367-2630/17/i2/a023015.